

THICKNESS EFFECTS IN HYDROGEN SORPTION OF  
MAGNESIUM/PALLADIUM THIN FILMS

A THESIS SUBMITTED TO  
THE GRADUATE SCHOOL OF NATURAL AND APPLIED SCIENCES  
OF  
MIDDLE EAST TECHNICAL UNIVERSITY

BY

AYSHE GHAREMESHG GHARAVI

IN PARTIAL FULFILLMENT OF THE REQUIREMENTS  
FOR  
THE DEGREE OF MASTER OF SCIENCE  
IN  
METALLURGICAL AND MATERIALS ENGINEERING

JANUARY 2012

Approval of the thesis:

**THICKNESS EFFECTS IN HYDROGEN SORPTION OF  
MAGNESIUM-PALLADIUM THIN FILMS**

submitted by **AYSHE GHAREMESHG GHARAVI** in partial fulfillment of the  
requirements for the degree of **Master of Science in Metallurgical and Materials  
Engineering Department, Middle East Technical University** by,

Prof. Dr. Canan Özgen  
Dean, Graduate School of **Natural and Applied Sciences** \_\_\_\_\_

Prof. Dr. Tayfur Öztürk  
Head of Department, **Metallurgical and Materials Engineering** \_\_\_\_\_

Prof. Dr. Tayfur Öztürk  
Supervisor, **Metallurgical and Materials Engineering Dept., METU** \_\_\_\_\_

**Examining Committee Members:**

Prof. Dr. Macit Özenbaş  
Metallurgical and Materials Engineering Dept., METU \_\_\_\_\_

Prof. Dr. Tayfur Öztürk  
Metallurgical and Materials Engineering Dept., METU \_\_\_\_\_

Assist. Prof. Dr. H. Emrah Ünalın  
Metallurgical and Materials Engineering Dept., METU \_\_\_\_\_

Assist. Prof. Dr. Y. Eren Kalay  
Metallurgical and Materials Engineering Dept., METU \_\_\_\_\_

Dr. Bilge İmer  
Military Electronics Industry (ASELSAN) \_\_\_\_\_

**Date:** \_\_\_\_\_ 25.01.2012 \_\_\_\_\_

**I hereby declare that all information in this document has been obtained and presented in accordance with academic rules and ethical conduct. I also declare that, as required by these rules and conduct, I have fully cited and referenced all material and results that are not original to this work.**

Name, Last Name: Ayshe Gharemeshg Gharavi

Signature :

## ABSTRACT

### THICKNESS EFFECTS IN HYDROGEN SORPTION OF MAGNESIUM/PALLADIUM THIN FILMS

Gharemeshg Gharavi, Ayshe  
M.Sc., Department of Metallurgical and Materials Engineering  
Supervisor: Prof. Dr. Tayfur Öztürk

January 2012, 50 pages

Magnesium (Mg) thin films with various thicknesses ranging from 50 to 1000 nm capped with nominally 20 nm Palladium (Pd) were prepared by a thermal evaporation unit. A total of 25 glass substrates were used in each experiment. The unit had a rotatable macro shutter, rectangular in shape, rotation axes opposite to the Mg source, which allowed controlled exposure of the substrates. Thin films of 50, 100, 150, 200, 300, 400, 500, 600, 800 nm and 1000 nm were produced in a single experiment. Hydrogenation and dehydrogenation of the films were examined using a gas loading chamber which allowed in-situ resistance measurement. Samples were hydrogenated isochronally up to 453 K with a heating rate of 1.5 K/min. Samples cooled to room temperature were subjected to dehydrogenation test. The chamber was taken under vacuum ( $\sim 10^{-2}$  mbar) and the sample was heated up to 453 K at a rate of 1.5 K/min. The results showed that the hydrogenation and dehydrogenation temperatures correlate with the film thickness, thinner films reacting with hydrogen at low temperatures. While 200 nm thin film hydrogenated at 420 K and desorbed it at 423 K, 50 nm thin film hydrogenated at room temperature and desorbed it at 405 K. Thicker films needed higher temperatures to react with hydrogen. It is concluded that films thinner than 200 nm react fully with hydrogen; while a considerable portion of the thicker films remain unreacted. Significance of this is discussed with reference to the design of hydrogen storage systems based on thin films or nanoparticles.

*Key words:* Magnesium thin films; Thermal evaporation; Hydrogen storage; Desorption temperature

## ÖZ

### MAGNEZYUM-PALADYUM İNCE FİLİMLERDE KALINLIĞIN HİDRÜR KARARLIĞINA ETKİSİ

Gharemeshg Gharavi, Ayshe  
Yüksek Lisans, Metalurji ve Malzeme Mühendisliği Bölümü  
Tez Yöneticisi: Prof. Dr. Tayfur Öztürk

Ocak 2012, 50 sayfa

Bu çalışma Magnezyum (Mg) esaslı ince filimlerin hidrojen ile tepkimesini konu almakta ve kalınlığın bu tepkimeye etkisini incelemektedir. Bu amaçla çalışmada 50-1000 nm arası farklı kalınlıklardaki filimler ısı buharlaştırma yöntemi ile üretilmiş ve her bir filim ince (20 nm) Pd ile kaplanmıştır. Farklı kalınlıktaki numuneler tek bir seferde bir makro gölgeleyici kullanılmak suretiyle üretilmiş ve 50, 100, 150, 200, 300, 400, 500, 600, 800,1000 nm kalınlığında fillimler elde edilmiştir. Filimlerin hidrojen alma ve verme özellikleri bir gaz yükleme odacığı kullanılmak suretiyle gerçekleştirilmiş ve reaksiyonun seyri elektriksel direnç ölçümü ile takip edilmiştir. Numuneler sabit hidrojen basıncı altında eşsürelili olarak hidrürlenmiş ve bu amaçla numuneler 1.5 K/dk hızla 453 K'e kadar ısıtılmıştır. Hidrojenin geri verilmesi benzer şekilde odacığın vakum altına ( $\sim 10^{-2}$  mbar) alınmasına takiben, oda sıcaklığındaki örneklerin aynı hızla 453 K'e ısıtılmasıyla takip edilmiştir. Elde edilen sonuçlar hidrürlenme ve dehidrürlenme sıcaklıklarının kalınlığa bağlı olarak değiştiğini göstermiştir. 200 nm'den ince filimlerin tamamen hidrürlendiği ve hidrojenini tamamen geri verdiği, her iki reaksiyonun nispeten düşük sıcaklıklarda gerçekleştiği tespit edilmiştir. 200 nm'den daha kalın filimlerde kısmi reaksiyon gözlenmiş ve artan kalınlıkla filmin önemli bir kısmının reaksiyona girmediği gözlenmiştir. Sonuçlar ince filimlerde 200 nm, parçacıklarda bu değerin iki katı 400 nm'nin hidrojen depolama açısından kritik değer olabileceğine işaret etmektedir.

*Anahtar Kelimeler:* Mgsnezyum ince film; Isıl buharlaştırma; Hidrojen depolama; Hidrojen alma; Hidrojen verme; Direnç ölçümü

## ACKNOWLEDGEMENTS

I owe my deepest gratitude to my supervisor **Prof. Dr. Tayfur Öztürk** for his guidance, collaboration and patience throughout the research.

My endless thanks and respect to **Prof. Dr. Naci Sevinç, Prof. Dr. Macit Özenbaş, Prof. Dr. M. Kadri Aydınol, Prof. Dr. İshak Karakaya, Prof. Dr. Bilgehan Ögel, Assist. Prof. Dr. H. Emrah Ünalın** and **Assist. Prof. Dr. Y. Eren Kalay** from whom I have taken courses throughout my MS studies.

My special thanks to **Dr. Hasan Akyıldız** for his endless support especially with experimental part of my thesis and for his illuminating guidance for the subject as a whole. Also, my thanks to **Çağla Özgıt** for her support initiating me to the subject.

I would also like to acknowledge my lab mates **Dr. Gülhan Çakmak, Dr. Serdar Tan, Zeynep Öztürk, Aslı Boran, Eren Şimşek, Fatih Pişkin, Burak Aktekin, Alptekin Aydınlı**.

My special thanks to **Mahmood Alipour Kanafi** for his endless moral supports. Thanks to my dear friends **Pantea Aurang, Naghme Sarfarazi, Nuriya Garipova, Özlem Taytaş**.

My special thanks to my mother **Ghorban Bakht** the dearest person in my life that without her I could not be what I am now. Thanks to my family members **Shahnaz, Shahram, Maryam** and **Hosseın** for their moral and financial supports.

I want to express my respect to my kind-hearted friend **Ali Rıza Akıncı** who gave me a chance to continue my education in Turkey. Also I want to remember **Celal Burak Oğuzhan** for his helps. Finally I would like to acknowledge Ministry of Education, Turkey for providing me scholarship to carry out this research.

# TABLE OF CONTENTS

ABSTRACT .....	<b>ERROR! BOOKMARK NOT DEFINED.</b>
ÖZ.....	v
ACKNOWLEDGEMENTS .....	vi
TABLE OF CONTENTS .....	vii

## CHAPTERS

1. INTRODUCTION.....	<b>Error! Bookmark not defined.</b>
2. LITERATURE REVIEW.....	3
2.1 Introduction.....	3
2.2 Thin Film and Bulk Effects on Sorption Properties.....	5
2.3 Nucleation Sites for Magnesium Hydride.....	6
2.4 (De)Hydrogenation of Mg/Pd Systems.....	9
2.5 Effects of Crystallinity .....	12
2.6 Effects of Grain Size .....	13
2.7 Effects of Alloying Elements.....	15
2.8 Hydrogen Blocking Layers .....	16
2.9 Effects of Film Thickness .....	19
3. EXPERIMENTAL .....	21
3.1 Materials.....	21
3.2 Substrate Cleaning .....	21
3.3 Thermal Evaporation.....	21
3.3.1 Thermal Evaporation Unit.....	21

3.3.2 Evaporation .....	23
3.4 Resistivity Measurement.....	23
3.4.1 Electrical Resistance in Mg/Pd Thin Films.....	23
3.4.2 Resistivity Measurement Setup.....	26
3.4.3 (De)Hydrogenation Experiments .....	28
3.5 Characterization of Thin Films .....	29
4.    RESULTS AND DISCUSSIONS .....	30
4.1. As-deposited State .....	30
4.2 Hydrogenated State.....	32
4.3 Dehydrogenated State .....	35
4.4 Microstructural Observations .....	39
5.    CONCLUSIONS.....	42
REFERENCES .....	44

## CHAPTER 1

### INTRODUCTION

Increasing the population of the world and restricted accessible fossil fuel reserves opened a new window for research on renewable energy sources such as wind, solar, hydroelectricity which are reputed as clean energy resources due to their less environmental side effects compared to the fossil fuels. Hydrogen plays a key role in renewable energy. Hydrogen can be stored in gas, liquid and solid forms. Hydrogen, when stored in liquid or gas form needs very stringent precautions especially for mobile applications. Hydrogen storage in the pressurized cylinder has quite low volumetric density and thus requires larger space for the same amount of hydrogen. Liquid hydrogen is not energy efficient since one third of the energy is used in liquefaction. On the other hand hydrogen storage in the solid state in the form of metal hydrides is quite safe and provides one of the most volumetrically efficient form of storing energy.

Among metal hydrides, magnesium hydride ( $\text{MgH}_2$ ) has high gravimetric and volumetric density for hydrogen (7.7 wt. %,  $55 \text{ kg/m}^3$ , Grau-Crespo et al. 2009). These properties make Mg a suitable medium for hydrogen storage material; but it suffers from two limitations which restricts its widespread application: *high thermodynamic stability of magnesium hydride* and *sluggish kinetics*.

Efforts to reduce the stability of  $\text{MgH}_2$  as well as to improve the kinetics of dehydrogenation concentrated on means of processing, yielding nanostructured materials. Ball milling of Mg with and without additives has been a common approach. An alternative approach is thin film processing which allows a better control of the resulting structure. It is known that thin films which are less than 100 nm can readily sorb hydrogen at room temperature; while films with one micron thickness behave like bulk samples. Films of intermediate thickness have been studied widely which display a mixed behavior (Akyıldız and Öztürk 2010).

In the current work, a systematic study was carried out on the thickness effects in sorption properties of Mg/Pd thin films. Mg films capped with Pd were deposited with thickness values ranging from 50 nm to 1000 nm and their hydrogenation and dehydrogenation properties were investigated. The study aims to establish a critical thickness value where thin-film-to-bulk transition takes place.

## CHAPTER 2

### LITERATURE REVIEW

#### 2.1 Introduction

Mg with an atomic number of 12 and hexagonal crystal structure is the seventh most abundant element in the earth's crust. It is impossible to find Mg in elemental form due to its very high reactivity with oxygen. A thin native oxide layer exists on its surface which restricts the Mg accessibility by limiting the diffusivity of the gases through the oxide layer. This metal is very light with a density of  $1.738 \text{ g/cm}^3$  in solid and  $1.584 \text{ g/cm}^3$  in liquid state at its melting point. Heat of fusion and vaporization of Mg are 8.48 and 128 kJ/mol respectively.

Properties such as low weight, high hydrogen capacity (7.7 wt. %) with the ability to form a hydride phase make Mg as a candidate for hydrogen storage material. When Mg is exposed to hydrogen gas a metal to insulator transition takes place and metallic Mg phase converted into  $\text{MgH}_2$ , a semiconductor material with a large band gap (nearly 5.6 eV). This phase transformation is accompanied with a change in crystal structure from hexagonal close packed (HCP) to body centered tetragonal (BCT) and significant changes in volume as well as in the transparency of the material.

Mg-H system suffers from two drawbacks that must be overcome before they can be used as storage material. The first is the high thermodynamic stability of magnesium hydride that comes from strong Mg-H bond strength. As a result of high heat of formation of bulk  $\text{MgH}_2$  in the vicinity of -75 kJ/mol (Krozer and Kasemo 1989) temperatures more than 573 K are needed for hydrogen desorption (Schlapbach and Züttel 2001) which is too high for practical storage purposes. Alloying Mg with other

metals such as nickel (Ni), aluminum (Al), yttrium (Y) will be helpful in decreasing the enthalpy of formation and desorption temperature but also it may decrease the storage capacity to some extent due to decreasing the amount of the storage material (Chacon et al. 2005 and Pasturel et al. 2006). Enthalpy of formation could be decreased by decreasing the size of the particulate material. According to Barcelo et al. 2010, this decrease is due to increased surface area associated with fine particles as well as the high fraction of grain boundary area in nanostructured materials.

The second drawback is the sluggish kinetics of sorption reactions of Mg-H systems. It originates from a number of sources: a native oxide layer on the particle surface, slow rate of dissociation of hydrogen on the surface and low diffusion rate of atomic hydrogen through the Mg and MgH<sub>2</sub> phases (Bouhtiyya and Roué 2009). According to Leon et al. 2002, parameters such as particle size, particle morphology and oxygen content have profound effects on sorption kinetics.

Sorption kinetics may be improved by mechanical milling technique which involves crushing the storage material using stainless steel balls under controlled atmosphere or cryogenic conditions creating new and fresh surfaces that are oxide free. This also introduces structural defects which enhance the kinetics of the sorption reactions (Zaluska et al. 1999). Easy insertion of catalysts into the particulate material is another advantage of mechanical milling which helps the hydrogen dissociation process (Singh et al. 2007).

Thin film processing is an alternative processing route which also improves the kinetics of sorption reaction. The most used deposition techniques are thermal evaporation, sputtering, electron beam evaporation and pulsed laser deposition (PLD). Thin film structures have large surface area for a given volume, which reduces the required diffusion distance. Insertion of a catalyst layer on the surface of the thin film is an easy process which improves the sorption kinetics. Depositing a layered structure will increase the sorption rates as a result of increasing the number of interfaces (Krozer and Kasemo 1987, Higuchi et al. 2002 and Qu et al. 2010).

## 2.2 Thin Film and Bulk Effects on Sorption Properties

Thin films differ from the bulk material due to the presence of mixed crystalline and/or amorphous phases, crystallite size, orientation and residual stresses resulting from film-substrate interface and nonstoichiometry (Pranevicius et al. 2009 and Dornheim et al. 2007).

The thick pure Mg thin film (30  $\mu\text{m}$ ), representative of bulk, was deposited on Si wafers by Leon et al. 2002 using thermal evaporation method. The film absorbed hydrogen at 623 K under 10 bar hydrogen pressure and reached to its maximum storage capacity of 7.5 wt. % within 1000 min. and desorbed it at the same temperature under a residual hydrogen pressure of 0.21 bar. Upon cycling, initial structure and morphology of the film was lost partially due to lattice expansion and contraction effect and numerous defects such as voids were created that facilitated the subsequent sorption reactions. Also as a result of high operating temperature, intermetallic compound  $\text{Mg}_2\text{Si}$  was detected at Mg/Si interface.

Barcelo et al. 2010 prepared nanostructured pure Mg thin films (2  $\mu\text{m}$ ) sandwiched between two Pd overlayers (20 nm) using PLD technique. Mean grain size of the film was 50 nm in as-deposited state and effect of substrate was removed by detaching the film. Absorption isotherms were measured from 10 mbar up to 2 bar at temperatures between 296 and 603 K. The formation enthalpy of magnesium hydride was -67 kJ/mol  $\text{H}_2$  which is to be compared with -75 kJ/mol  $\text{H}_2$  for the bulk material. The decrease in enthalpy value explained within the concept of excess volume. According to Barcelo et al. 2010, PLD technique is particularly important in creating excess volumes and the method therefore would be a proper alternative for high energy ball milling to produce the destabilized hydrogen storage materials.

Nanostructured Mg thin films of 100 nm thickness covered with 10 nm Pd overlayer prepared by Ingason and Olafsson 2005 using sputter deposition. Resistance measurement method was used to monitor both the growth and the stability of the deposited films. In-situ hydrogenation experiments carried out between 333 and 373 K and resistance isotherms were plotted at different temperatures and pressures. The

stability of MgH<sub>2</sub> was similar to Mg which was produced with ball milling. There was also difficulty in full hydrogenation of the film. This was attributed to the formation of MgH<sub>2</sub> layer at the Pd/Mg interface which prevented further diffusion of hydrogen into Mg.

### 2.3 Nucleation Sites for Magnesium Hydride

MgH<sub>2</sub> formation and decomposition follows nucleation and growth mechanism (Qu et al. 2009). The number of nucleation sites depends on the number of interfaces and the method of film preparation. According to Ryden et al. 1989, hydrogen atoms at hydrogenation process prefer to occupy the host Mg sites close to Pd overlayer and hydride phase starts to nucleate at Pd/Mg interface. Spatz et al. 1993 used vacuum evaporation method for deposition of pure Mg layers (2-80 nm) on pre-hydrated Pd foils as atomic hydrogen resource to eliminate the slow diffusion of gaseous hydrogen on Mg surface. MgH<sub>2</sub> phase nucleated at PdH<sub>x</sub>/Mg interface and formed a barrier layer immediately which prevented the further diffusion of hydrogen. They reported an overall diffusion coefficient of  $D_H = 1.1 \times 10^{-20} \text{ m}^2/\text{s}$  in the film at 305 K.

Vermeulen et al. 2009 used Electron beam evaporation method for deposition of Mg(200 nm)/Pd(10 nm) thin films on quartz substrates. Sorption experiments were carried out at room temperature electrochemically. During desorption process, Mg crystallites start to nucleate at MgH<sub>2</sub>/Pd interface and slow diffusion of hydrogen through the Mg layer determined as rate limiting step for dehydrogenation process. Enthalpy of formation and decomposition of MgH<sub>2</sub> was reported as -72 and -74 kJ/mol H<sub>2</sub>, respectively.

Singh et al. 2007 prepared nearly 1 μm thick pure Mg thin films covered with 100 nm Pd overlayer using sputter deposition and PLD techniques on silicon (Si) substrate. After hydrogenation treatment, cross sectional investigations showed that the sputter deposited samples consisted of one MgH<sub>2</sub> layer while in PLD deposited samples had two layers; nearly 150 nm fully hydrogenated MgH<sub>2</sub> layer in the interface of the Mg/Si and an intermediate layer composed of MgH<sub>2</sub> crystallites, amorphous Mg, MgH<sub>2</sub> and

MgO on top. The formation of two layer structure was attributed to the nature of PLD method which favours the formation of non-equilibrium films with higher defect density. Defects have relatively open structure with respect to other parts of the film and make the hydrogen diffusion easier towards the Mg/Si interface and MgH<sub>2</sub> starts to nucleate there. Optimum hydrogenation condition (4-7.5 wt. % H<sub>2</sub>) achieved at hydrogen pressure of 0.25 - 1.0 MPa at ~470 K for both techniques.

Efficiency of Mg-H system is affected by the number of Pd/Mg interfaces that participate in sorption processes and is the dominant factor in improving the sorption properties. Three layered Pd(15 nm)/Mg(170 nm)/Pd(15 nm) thin films using PLD method were prepared on Ni discs by Bouhtiyya and Roué 2009, in the presence of different pressures of helium (He) gas. Surface roughness and porosity of Mg layer increases with increasing the He gas pressure which extends the Pd/Mg interface and it is the main reason for amending the sorption properties. At lower He gas pressures crystallinity of the film decreased but electrochemical hydrogen sorption properties of the films did not improve. This shows the importance of Pd overlayer more than Mg crystalline structure. Similar conclusions were reached by Paillier and Roue 2005 which studied Mg/Pd (total thickness of 27 and 330 nm) thin films under different deposition atmosphere (vacuum, He and Ar) with PLD method.

Higuchi et al. 2002 prepared Pd(50 nm)/Mg(25-800 nm)/Pd(50 nm) thin films using radio frequency (RF) magnetron sputtering technique. H/Mg ratio in three layered Pd/Mg/Pd film was about two times larger than that in two layered Pd/Mg structure. Qu et al. 2010 sputter deposited two kinds of film; two layered Mg(100 nm)/Pd(10 nm) and three layered Pd(5 nm)/Mg(100 nm)/Pd(5 nm) thin films and compared their structural, optical and electrical properties. Hydrogenation carried out at 353 K in sodium borohydride (NaBH<sub>4</sub>) solution and dehydrogenation at ambient temperature in air or in hydrogen peroxide (H<sub>2</sub>O<sub>2</sub>) solution. Like Higuchi's study, again three layered thin film exhibited better sorption properties compared to the two layered thin films. Qu attributed this to the action of Pd clusters as heterogeneous nucleation sites for hydride phase. The overall activation energy for hydriding was 80 and 60 kJ/mol for two layered and three layered thin films respectively. Kumar et al. 2009 prepared bare

Mg(250 nm) and Pd(10 and 40 nm) coated Mg(250 nm) thin films on Si and glass substrates using thermal evaporation technique for Mg layer and electron beam evaporation method for Pd deposition. Hydrogenation of the films carried out under 0.15 MPa of H<sub>2</sub> gas in the temperature range of 323-423 K for 0.5-5 h. The films were able to absorb 6.0-7.0 wt. % H<sub>2</sub>. Dehydrogenation experiments were carried out under vacuum condition at 373 K for 3 h. While pure Mg thin films did not absorb hydrogen, non-stoichiometric hydride phase formation started at Mg/Pd interface successfully in the case of Pd coated Mg films. The hydride proceeds further into the interiors of the film and reached to 300 nm thickness at 348 K with 55 at. % hydrogen content. Thickness of the hydride layer and H<sub>2</sub> content increased with increasing the absorption temperature and soaking time at that temperature. This also increased the room temperature stability of MgH<sub>2</sub>. Hydrogen diffusion coefficient (D<sub>H</sub>) for hydride phase was  $1.7 \times 10^{-20}$  m<sup>2</sup>/s at 323 K.

Kelekar et al. 2007 prepared pure Mg(400 and 800 nm) thin films covered with Pd(25 nm) using sputter deposition method on aluminium oxide (Al<sub>2</sub>O<sub>3</sub>), lithium gallate (LiGaO<sub>2</sub>), and glass substrates. Epitaxial growth of Mg and sorption kinetics of the film was investigated using x-ray diffraction (XRD) and resistance measurement methods. Hydrogenation properties carried out under 0.6 MPa hydrogen pressure at 373 K for four days and dehydrogenation experiments have been done at 355 K in air. Depending on the used substrate, MgH<sub>2</sub> grows epitaxially according to MgH<sub>2</sub>(110)[001]//Mg(001)[100] and MgH<sub>2</sub>(200)×[001]//Mg(110)[-111] relationships for Al<sub>2</sub>O<sub>3</sub> or LiGaO<sub>2</sub> respectively. On glass substrate, hydride grows in typical direction of (110). At dehydrogenation, crystalline quality of re-grown Mg is an indication of the place where Mg starts to “re”-crystallize. In the case of Al<sub>2</sub>O<sub>3</sub> a portion of reacted Mg begins to re-crystallize at the MgH<sub>2</sub>/Mg interface by solid phase epitaxy mechanism while the rest re-crystallize at Pd/Mg interface following nucleation and growth mechanism. The fraction of Mg that was re-grown epitaxially depends on the thickness of the hydride layer. At fully hydrogenated films due to the absence of a continuous epitaxial layer of unreacted Mg, negligible amount of Mg was able to re-grow epitaxially. The best result for hydrogenation was achieved for glass substrates.

Lohstroh et al. 2004 prepared  $\text{Mg}_2\text{Ni}$ (30-300 nm) thin films using magnetron co-sputtering on quartz, glass substrates covered with calcium fluoride ( $\text{CaF}_2$ ) and indium tin oxide (ITO). The films were capped with Pd(5-25 nm). Hydrogenation of the films carried out in-situ at pressures up to 1 bar  $\text{H}_2$ . Dehydrogenation of the films carried out at 373 K in air. The results showed that  $\text{Mg}_2\text{NiH}_{4.8}$  phase preferentially nucleates at the film/substrate interface and not close to the catalytic Pd capping layer.

#### **2.4 (De)Hydrogenation of Mg/Pd Systems**

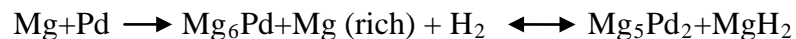
In Mg-Pd systems, the formation of phases such as  $\text{MgH}_2$ ,  $\text{Mg}_6\text{Pd}$ ,  $\text{Mg}_5\text{Pd}_2$  and  $\text{MgO}$  may restrict hydrogen diffusion and can result in partial (de)hydrogenation which might decrease the efficiency of the system by a considerable extent. Then, it is necessary to probe the properties of these phases and their effects on sorption reactions.

Gautam et al. 2011 prepared Pd capped Mg(500 nm) thin films on glass substrates using magnetron sputtering method. Absorption experiments were carried out at 473 and 523 K for 12 h under 2 bar hydrogen pressure and desorption tests were carried out at 523 K for 1 h and 673 K for 6 h under vacuum condition. Upon hydrogenation,  $\alpha$ - $\text{MgH}_2$  (at 473 K),  $\gamma$ - $\text{MgH}_2$  (at 523 K) and  $\text{Mg}_5\text{Pd}_2$  phases have been detected and the dehydrogenation process was not complete even at 673 K. Also a phase transformation from  $\alpha$ - $\text{MgH}_2$  to  $\gamma$ - $\text{MgH}_2$  was detected at 523 K. Westerwaal et al. 2008 prepared  $\text{MgH}_2$  layer (180 nm) with very high purity (with resistance value of infinity) in situ, using activated reactive evaporation (ARE) method. End part of a high temperature optical fiber was used as the substrate. After deposition of Pd overlayer, hydrogen started to release from as-grown  $\text{MgH}_2$  film and small isolated Mg impurities formed inside the hydride layer. When the sample re-loaded with hydrogen gas, the film behaved like an ex-situ hydrogenated Mg thin film. Distribution of Mg phase changed drastically which formed an electrically percolating network throughout the  $\text{MgH}_2$  film at grain boundaries that causes to returning the resistance of the film to the normal observed values of 10 m $\Omega$ .

Siviero et al. 2009 sputter deposited Mg(200 nm)/Pd(5-10 nm) thin films on Si and glass substrates. Nearly pure hydrogen gas at 1 bar has been used for hydrogenation at 373 K for 5.5 h. XRD experiments revealed two forms of magnesium hydride;  $\alpha$ -MgH<sub>2</sub> (tetragonal) and  $\gamma$ -MgH<sub>2</sub> (orthorhombic). Formation of metastable  $\gamma$ -MgH<sub>2</sub> attributed to expansion of the film during hydrogenation that imposes compressive stresses and clamping of the film to the substrate. Original texture of the film was lost upon dehydrogenation process in air at temperature range of 333-373 K for 2 h even after the first cycle. Degradation of the Pd overlayer and subsequent oxidation of the surface was established as the main reason of decreasing the sorption efficiency upon cycling. Desorption of hydrogen took place at temperatures higher than 423 K.

Tamboli et al. 2010 prepared post oxidized crystalline and amorphous Mg(300, 450 and 600 nm) thin films on glass substrates. Adhesion, porosity and intrinsic stress of the films increased with increasing the oxidation temperature (573, 623 and 673 K) and duration (90 and 180 min.); whereas adhesion increased and intrinsic stress decreased slightly with increasing the film thickness.

Ye et al. 2010 prepared 33 layered Mg/Pd sandwich-like structure thin film on Si wafer using sputtering method. The thickness of each Mg and Pd layer was 470 nm and 80 nm respectively. Before hydrogenation test, the sample was activated under 30 bar hydrogen pressure at 473 K for 4 h. Absorption experiments were carried out at room temperature, 323 and 373 K. Maximum hydrogen absorption capacity did not change significantly with increasing the temperature. Upon cycling, multi-layered structure of the film was lost and composition of the film changed with alloying of Mg and Pd along the Pd/Mg interfaces even at low temperatures. Sorption reactions took place according to the following chemical reaction;



During hydrogenation, Mg<sub>6</sub>Pd formed first, followed by MgH<sub>2</sub> and Mg<sub>5</sub>Pd<sub>2</sub>. After desorption, Mg<sub>6</sub>Pd and Mg<sub>5</sub>Pd<sub>2</sub> phases were detected that showed the complete dehydrogenation of the film at 323 K. High interfacial energy was established as the driving force for the formation of Mg<sub>6</sub>Pd phase and as the cause of the instability of the

multi-layered thin film. The interface free energy of Mg/Pd in as-deposited state was reported to be -2.34 kJ/mol.

In order to investigate the intermixing and formation of Mg/Pd intermetallics, Reddy et al. 2009 prepared Pd(10 and 50 nm)/Mg(300 nm) thin films on Si substrates. Thermal evaporation method was used for deposition of Mg layer and electron beam evaporation method for deposition of Pd layer. The samples were annealed under vacuum condition at a temperature range of 348-473 K for 1-8 h and then hydrogenated at 348 and 473 K under 1.5 bar hydrogen pressure for about 4 h. During annealing under vacuum condition, Mg<sub>6</sub>Pd or Mg<sub>5</sub>Pd<sub>2</sub> intermetallic phases were formed while in annealing under hydrogen, these phases did not form. Films with 10 nm Pd layer showed higher extent of interaction. Mg<sub>6</sub>Pd phase formed at both Pd thicknesses and its quantity increased with increasing the annealing temperature; while Mg<sub>5</sub>Pd<sub>2</sub> phase formed upon annealing for 5 h in Pd(50 nm)/Mg(300 nm)/Si films. The diffusion of Pd into Mg grain boundaries was the major cause of Mg<sub>6</sub>Pd phase formation and intermixing started from the interfacial regions.

Hydrogen storage properties of multi-layered Mg(200 nm)/Pd(50 nm) thin films prepared by magnetron sputtering method was investigated by Fujii et al. 2003. In the case of thin film, seven layers of Pd and Mg were deposited consecutively with increasing the number of layers, thermal desorption spectroscopy (TDS) peak position shifted to lower temperatures and the film was able to store ~5 mass. % H<sub>2</sub> at 373 K under 0.1 MPa H<sub>2</sub> pressure. The film was dehydrogenated fully at 360 K under vacuum condition. By preparing a three layered Pd(10 nm)/Mg(800 nm)/Pd(10 nm) thin film, Fujii showed that the total content of hydrogen was independent of Pd layer thickness.

Qu et al. 2010 prepared three layered Pd(5 nm)/Mg(100 nm)/Pd(5 nm) thin films on silicon wafer, glass and ITO-coated glass substrates using the magnetron sputtering method. He investigated the structural, optical and electrical properties of the films. Hydrogenation experiments carried out with nearly pure hydrogen gas at room temperature for 4 h and dehydrogenation tests were conducted in dry air at different temperatures. By simulating and modeling the resistance data, Qu showed that desorption process follows a nucleation and growth mechanism. In addition, they found

a value of 48 kJ/mol for activation energy of hydrogen diffusion. The hydrogen diffusion coefficient was  $D_H: 8 \times 10^{-15} \text{ Cm}^2/\text{s}$  at 298 K. Small activation energy and fast hydrogen diffusion rate were attributed to the cooperative interaction of Mg and Pd layers and extended Pd/Mg interfaces.

## 2.5 Effects of Crystallinity

Four types of Pd(25 nm)/Mg(200 nm) thin films with different degree of crystallization for Mg layer were sputter deposited on glass substrates by Higuchi et al. 1999. Hydrogenation of the films carried out in situ under 0.1 MPa hydrogen pressure at 373 K for 24 h and dehydrogenation experiments conducted under vacuum condition. The hydrogen capacity of the films did not change significantly but desorption temperature of the films shifted to lower values with decreasing the crystallinity. The lowest desorption temperature of ~463 K was obtained for a film with the lowest crystallinity. This particular film contained 5.6 mass. %  $\text{H}_2$ .

Akyıldız and Öztürk 2010 co-deposited 300 nm Mg-Cu thin films in crystalline and amorphous state, coated with Pd(10-25 nm) overlayer on glass substrates. They systematically varied the Cu content and the films were deposited at two different temperatures (298 and 223K) using thermal evaporation method. Desorption temperature was reduced down to 333 K for  $\text{Mg}_{85}\text{Cu}_{15}$ . Decreasing the deposition temperature favoured the amorphous structure so films co-deposited at 223 K were amorphous while the films deposited at room temperature had crystalline structure. By increasing the Cu content of the film or decreasing the temperature of the substrates, sorption temperatures decreased significantly due to the refinement of the film's structure. The film with the amorphous structure was able to store the highest hydrogen content.  $\text{Mg}_{90}\text{Cu}_{10}$  was suggested as the hydrogen storage medium with 5.9 wt. % hydrogen content in near ambient condition.

Qu et al. 2009 studied the effect of annealing temperature on the morphology and structure of sputter deposited 100 nm Mg thin films on Si (100) and glass substrates which were coated with 10 nm Pd overlayer. Hydrogenation process carried out at room

temperature and 353 K and dehydrogenation carried out at 353 K. Samples which were annealed at 473 K for 2 h demonstrated the best sorption properties. Higher annealing temperatures promoted the crystallinity of the films. In addition, Qu suggested that this leads to the reduction of the hydrogen diffusion rate due to oxidation of the surface and grain growth effect at higher annealing temperatures.

Özgit et al. 2010 prepared Mg(350 nm)/Pd(6 and 48 nm) thin films on glass substrates using thermal evaporation method. Hydrogenation experiments carried out under two different conditions; isothermal condition with changing the pressure of hydrogen gas up to 10 bar and isochronal condition under 1 bar hydrogen pressure with a slow heating rate from room temperature till 453 K. MgH<sub>2</sub> phase formed under isothermal condition had a random texture while under isochronal condition textured MgH<sub>2</sub> was formed in the temperature range of 381-443 K. MgH<sub>2</sub> phase grew in (110) direction due to the tendency of the system to minimize the in-plane lattice distortion.

## **2.6 Effects of Grain Size**

Zaluska et al. 1999 prepared nanostructured Mg powder using ball milling method and showed that decreasing the particle size down to a few nanometers could decrease the operating temperature of the system significantly. The sorption kinetics would also be improved. These improvements were attributed to three reasons; i) formation of numerous defects and grain boundaries near the powder surface which favours the nucleation of the hydride phase, ii) presence of grain boundaries and defects which facilitate the formation of hydride phase in places far from the surface and iii) multi-crystal structured magnesium hydride that provides easy path for hydrogen diffusion. Also Zaluska showed that addition of trace amount of elements such as vanadium (V), zirconium (Zr) and mixture of Mn-Zr is more effective than Pd or Fe in improving the sorption kinetics. It was also observed that the equilibrium pressure of Mg could be shifted to higher values by addition of yttrium (Y) and zinc (Zn).

Yamamoto et al. 2002 studied optical and structural properties of pure Mg(200 nm) thin films protected with Pd(10 and 50 nm) overlayer. The films were deposited on glass and

quartz substrates using sputter deposition method. Absorption experiments were carried out in an in-situ system under hydrogen pressure of 0.1 MPa at 373 K for 24 h. Desorption tests carried out ex-situ and the films were therefore exposed to air. In as-deposited state, Mg layer was composed of columnar grains with c-axis perpendicular to the film with width less than 100 nm. Upon hydrogenation, shiny mirror-like Mg (001) was converted to transparent MgH<sub>2</sub> (hk0). The films were partially hydrogenated and stored 6 mass. % H<sub>2</sub>. After the first cycle, the columnar grains were restructured to grains of 50-100 nm in diameter. In addition, heating the films above 453 K increased the risk of formation of Mg<sub>6</sub>Pd phase at Mg/Pd interface.

Qu et al. 2009 sputter deposited Mg(100 nm)/Pd(10 nm) thin films on Si, glass and ITO coated glass substrates. The samples fully hydrogenated under 0.1 MPa hydrogen pressure at 353 K for 4 h and the films lost all their hydrogen content when exposed to air at 298 K. Upon cycling, grain size of the Mg phase decreased due to the strong hydrogen induced stresses during the structure change from hcp-Mg to rutile type MgH<sub>2</sub>. This reduction in grain size and formation of more defects improved the sorption properties at subsequent cycles. Qu reported an activation energy ( $E_a$ ) value of 67 kJ/mol for H<sub>2</sub> diffusion in desorption and  $D_H$  was  $6.52 \times 10^{-15} \text{ cm}^2 \text{ s}^{-1}$  at 298 K.

Sunitha et al. 2009 prepared two layered Mg(300 nm)/Pd(10 and 50nm) thin films on Si substrates. Thermal evaporation method was used for the deposition of Mg and electron beam evaporation was used for Pd deposition. Grain boundary diffusion coefficient was calculated as  $1.4 \times 10^{-11} \text{ cm}^2/\text{s}$  that was about six orders of magnitude greater than lattice diffusivities at 473 K. Annealing temperatures higher than 473 K caused the alloying of Mg with substrate. Thus, it was necessary to limit the desorption temperatures less than 473 K to avoid losing the storage material and to prevent the depletion of Pd overlayer. Diffusion onset temperature at Mg/Pd interface depended on the thickness of Pd overlayer. They suggested that insertion of a buffer layer, allowing hydrogen diffusion, between the Mg and Pd layers would be a good remedy for interdiffusion of the neighboring layers.

## 2.7 Effects of Alloying Elements

Richardson et al. 2003 prepared co-sputtered Mg-(Ni,Co and Ti) thin films on Si and silicon nitride substrates. XRD and X-ray absorption spectroscopy experiments were carried out in-situ. Hydrogenation led to large changes in both reflectance and transmittance of the films. Mg K-edge and Ni, Co and Ti L-edge spectra were measured which reflects both reversible and irreversible changes in the metal environments. A significant shift in the nickel L absorption edge showed that it would be an active participant in hydride formation. The effect of cobalt and titanium was much less dramatic, suggesting that these metals act primarily as catalysts for  $MgH_2$  formation.

Ferrer et al. 2007 prepared multi-layered Pd/Fe(Ti)/Mg-Al/Mg/Fe(Ti)/Pd thin films using electron beam physical vapour deposition on bare and photoresist-coated Si wafers. They changed the ratio of Al/Mg and deposited a thin layer of Fe or Ti between Pd and Mg, so as to make use of possible catalytic effect of these elements and to avoid the formation of  $Mg_xPd_y$  alloy. Four probe resistivity measurement and differential scanning calorimetry technique were used for probing the hydrogenability of the films and its reaction kinetics. Results were compared with pure Pd/Mg/Pd thin films. Aluminum (Al) had a positive effect on hydrogenation properties but did not significantly decrease the desorption temperature. Titanium (Ti) was more effective than iron (Fe) as a buffer layer. Disadvantage of Ti was that the film was detached from the surface as a result of bubble formation.

Akyıldız et al. 2006 prepared pure Mg(420 nm), Au-Pd capped Mg(1400 nm), co-deposited Mg-Cu(570 nm) and multi-layered Mg-Cu(1500 nm) films on glass substrates using thermal evaporation method. In as-deposited state the films were composed of columnar grains with some degree of preferred orientation. The films were hydrogenated under 10 bar hydrogen pressure by changing the temperature and time for each film system. Multi-layered Mg-Cu system exhibited the best result for hydrogen storage purposes and nearly all the Mg was converted into hydride phase at 473 K. Akyıldız suggested that there is a narrow temperature interval for successful hydrogenation process. This is in such a manner that at the upper end of this interval the internal reactions are dominant while at the lower end, the kinetics of hydrogenation

was too slow for the reaction to be complete. 473 K was determined as the working temperature for the mentioned film systems.

Pasturel et al. 2006 successfully hydrogenated sputter deposited Pd doped Mg thin films ( $\text{MgPd}_y$ ,  $0.023 < y < 0.125$ ) on glass substrates with 10 nm Pd overlayer. Upon hydrogenation under 0.5 bar hydrogen at room temperature, thickness, electrical resistivity and rate of hydrogenation of the films increased by the increased doping of Pd. However, increased doping results in the reduction of its total transmittance. Optical band gap ( $E_g$ ) decreased linearly with increasing doping of the film.

## 2.8 Hydrogen Blocking Layers

Krozer and Kasemo 1987 prepared Pd(5-10 nm)/Mg(380-780 nm) thin films on the gold electrode of a quartz crystal microbalance (QCM) as the substrate. The films were hydrogenated at 293 K in the pressure range of 0.03-60 Torr. Hydrogen uptake of the films was estimated by measuring the mass change of the QCM. The results showed an unusual kinetical behavior of Pd/Mg films; (i) saturation of hydrogen uptake took place far from the stoichiometric  $\text{MgH}_2$  at room temperature and (ii) increasing the hydrogen pressure decreased the saturation uptake significantly. They attributed this to the formation of hydride at Mg/Pd interface. To verify the formation of hydride phase at the interface, they prepared Pd(7 nm)/Mg(300 nm)/Pd(15 nm)/Mg(300 nm) thin film. The saturation uptake of this structure was more than two times the previous case. They further argued that the presence of vacancies or vacancy pairs, would act as the trap for hydrogen atoms. During hydriding process, concentration of hydrogen at the interface increases and reaches a critical value which leads to nucleation of hydride phase. Subsequently the hydride phase grows along the interface. Lattice expansion during the hydriding leads to further lowering the electron density down to where a coherent interface hydride forms. At this point the hydriding virtually stops because of low diffusion coefficient through the hydride phase. At higher hydrogen pressures, the concentration of hydrogen in Pd layer becomes larger which leads to the interface hydride formation at a smaller total hydrogen uptake. The hydride formation then

saturates with a lower concentration of hydrogen in the Mg bulk at higher pressures which explains the negative pressure dependence. H<sub>2</sub> diffusion through the hydride phase was determined as the rate limiting step. Also they mentioned that the film thickness does not have a significant effect on the total hydrogen uptake.

In a similar study, Krozer and Kasemo 1989 prepared Pd(7.5 nm)/Mg(800 nm) thin film. After hydrogenation of the films, the samples were de-hydrated under vacuum at 330 K. They defined a working space in the temperature range of 260-360 K and pressure range of 0.03-30 Torr, where equilibrium data for Mg-H system were obtained. Hydride formation temperature was defined as the lower limit which was pressure dependent and the formation of Mg/Pd alloy was determined as the upper limit. At very low pressures, equilibrium takes very long time to be achieved due to the low uptake rate. At very high pressures hydrogenation takes place very fast and released heat due to the exothermic hydride formation makes measurements difficult under isothermal condition. Thus, it was necessary to keep the pressure at moderate values. Enthalpy of hydriding and dehydriding of the films was  $60.7 \pm 6.3$  and  $71.2 \pm 4.2$  kJ/mol H<sub>2</sub> respectively.

Kelly and Clemens 2010 prepared epitaxially grown Mg(200, 400 and 800 nm) thin films covered with 25 nm Pd overlayer on Al<sub>2</sub>O<sub>3</sub> (0001) single crystal substrates. They hydrogenated the films under 5.5 and 5.7 bar H<sub>2</sub> pressure at 393 and 398 K. In-situ XRD method was used to examine the kinetics of hydride formation. Extracted data were successfully compared with the Deal-Grove model for the oxidation of silicon where the hydride growth in these films proceeds with a kinetics that is compatible with moving planar interface growth. For the conditions examined, hydrogen diffusion through the growing hydride layer controlled the growth rate for hydride layer for thicknesses above ~60 nm. For thinner layers, the control was exercised by the reactions at an interface or diffusion through the fixed Pd layer.

Oguchi et al. 2010 prepared a wedge-shaped Mg<sub>98.4</sub>Ti<sub>1.6</sub> thin film with a thickness gradient started from 0 nm up to ~500 nm on 1 cm-long Al<sub>2</sub>O<sub>3</sub> (0001) single crystal substrate coated with 5 nm Pd overlayer using electron beam deposition method. Hydrogenation process carried out under 0.3 MPa hydrogen pressure at 373 K for 1 h.

IR imaging method (optical method) was used to determine the thickness and rate of heterogeneous growth of hydride phase. Initial growth rate of the hydride phase was determined as  $\sim 1.3$  nm/s and this rate decreased to  $\sim 0.03$  nm/s due to the formation of a blocking hydride layer. According to transmission electron microscopy (TEM) observations, hydride phase started to nucleate from the surface, beneath the Pd overlayer, and proceed towards the substrate. Oguchi detected  $\sim 120$ - $150$  nm hydride phase with TEM images and recommended that the film thickness ought to be less than  $150$  nm for complete hydrogenation.

Hjort et al. 1996 studied the effect of oxygen in Mg/MgO<sub>x</sub> interface of a multilayered Pd/Mg thin film. A thin oxide layer (oxygen concentration in MgO<sub>x</sub> is less than  $160$  ng/cm) increased the hydrogen uptake as compared to pure Mg/Pd thin films while at higher thicknesses it decreased the sorption rate significantly. Total hydrogen storage capacity decreased in films with both thin and thick oxide layer. They also mentioned that even very thick oxide layers did not block the hydrogen diffusion completely.

Electron beam evaporation method was used by Ostefeld and Chorkendorff 2006 for preparation of  $7$  nm Mg thin film on Mo (111) substrate and subsequently capped with stoichiometric MgO overlayer ( $2.6$  nm) by post oxidation of Mg layer. Oxide layer on the surface acted as a cap and prevented the Mg loss at high desorption temperatures and postponed the H<sub>2</sub> desorption to higher temperatures. Upon applying the oxide layer, the desorption temperature shifted to higher temperatures and “apparent desorption energy” of the film increased from  $146$  kJ/mol to  $314$  kJ/mol upon post-oxidation.

Ostefeld et al. 2007 prepared  $40$  nm Mg thin films on Mo (111) single crystal and coated it with  $0.05$  nm thick Pt overlayer using the same deposition method. Pt catalyst increased the hydrogen uptake significantly even at room temperature and decreased the influence of self blocking effect caused by absorbed H<sub>2</sub>. It is necessary to mention that while stoichiometric MgO film on the surface blocks the hydrogen diffusion, non-stoichiometric and post oxidized MgO<sub>x</sub> layer was still permeable to H<sub>2</sub> gas.

## 2.9 Effects of Film Thickness

Ares et al. 2010 deposited crystalline Mg thin films with two different thicknesses (100 and 300 nm) covered with 10 nm Pd overlayer using electron beam evaporation method. Decomposition of MgH<sub>2</sub> films occurred at T<sub>d</sub> ~ 421 K under air and the process seems to be controlled by a bidimensional interphase mechanism with activation energy of 135±20 kJ/mol H<sub>2</sub> that was close to that of milled bulk Mg. The desorption process was not complete even for thinner films. They concluded that the film thickness and crystallite size did not affect the desorption temperature significantly.

Shalaan and Schmitt 2006 sputter deposited pure Mg(100, 200 and 300 nm) thin films in nanoscale and polycrystalline forms coated with 15 nm Pd overlayer on glass substrates. Upon hydrogenation, polycrystalline films did not show any sign of hydrogenation; but in the case of nanoscale Mg films, optical switching time decreased with decreasing the thickness of the films at room temperature and 1 bar H<sub>2</sub> pressure. They attributed this to the nano nature of the films due to the enhanced surface area, large concentration of the defects and increasing the reactivity in nano scale.

Qu et al. 2010 prepared Mg(20-100 nm)/Pd(5 nm) pure Mg thin films deposited on Si wafer and glass substrates using magnetron sputtering method. Absorption experiments were carried out in the temperature range of 298-338 K under  $7 \times 10^4$  Pa of H<sub>2</sub> pressure. Decreasing the film thickness significantly increased the H<sub>2</sub> diffusion coefficient, H<sub>2</sub> absorption flux and the film's absorption kinetics. The thinnest film absorbed 5.5 wt. % H<sub>2</sub> at 298 K. Maximum MgH<sub>2</sub> layer's thickness was not more than 50 nm. Therefore to obtain a fully hydrided film, the thickness of the film must be less than 50 nm otherwise the risk of partial hydrogenation increases significantly. MgH<sub>2</sub> layer thickness increased with temperature and with decreasing the H<sub>2</sub> pressure. H<sub>2</sub> diffusion coefficients of the films were determined electrochemically in 6 M potassium hydroxide (KOH) solution using counter and reference electrodes Pt foil and Hg/HgO respectively. Diffusion coefficients were much faster than the bulk value ( $1.1 \times 10^{-16}$  cm<sup>2</sup>s<sup>-1</sup>) at 300 K. H<sub>2</sub> diffusion coefficients increased with a decrease in the film

thickness that was attributed to the smaller amount of the inner MgH<sub>2</sub> layer and shorter diffusion distance.

Yoshimura et al. 2004 prepared Mg(60, 120 and 250 nm)/Pd(4 and 10 nm) thin films on Si substrates using magnetron sputtering method. Hydrogenation of the films carried out with 4 % H<sub>2</sub> gas diluted with argon at room temperature. Drastic optical changes occurred within 5 s in the films and reflectance percentage had a direct relationship with the thickness of the film. They established that an intermixing layer forms near Mg/Pd interface so that hydrogenation in this layer occurs very fast. The sputter deposition method used in this study was proposed to be effective in fast hydrogenation and formation of intermixing layer due to its non-equilibrium nature.

Higuchi et al. 2002 prepared sputter deposited three layered Pd(50 nm)/Mg(25-800 nm)/Pd(50 nm) thin films on glass substrates. Hydrogenation of the films carried out in-situ at 373 K for 24 h under 0.1 MPa H<sub>2</sub> pressure. Upon absorption, the films stored nearly 5.0 mass. % H<sub>2</sub> and this value was independent of the film thickness. TDS method was used for measuring the desorption properties and the samples heated from room temperature to 773 K. The results showed that with increasing the film thickness, desorption temperature of the films shifts towards the lower values. The least desorption temperature of 360 K was obtained for the thickness of 800 nm. For clarifying this unusual event, they proposed that the thicker Mg layer are fully hydrogenated and peel off from the substrate. Stored H<sub>2</sub> at Pd becomes unstable and H<sub>2</sub> desorption takes place at both sides of the Pd/Mg/Pd thin film that imposes compressive stress on the Mg layer. This compressive stress destabilizes the hydride phase and causes it to desorb H<sub>2</sub> at low temperatures. They called this dehydrogenation scenario as “cooperative phenomena”. This hypothesis to be applicable, the film must be detached from the substrate. This does not occur for Mg/Pd or thinner Pd/Mg/Pd films. Also the width of Mg columns is smaller for three layered Pd/Mg/Pd thin films which increases the amount of grain boundaries as compared to two layered Mg/Pd films. This makes H<sub>2</sub> diffusion easier for the former films. As a whole, three layered Pd/Mg/Pd thin films showed better sorption properties as compared to two layered Pd/Mg structure.

## CHAPTER 3

### EXPERIMENTAL

#### 3.1 Materials

Materials used for film deposition were Mg granules (*Alfa Aesar* 99.98% pure, -4 mesh) and Pd (*Kurt J. Lesker* 99.95 % pure, 3 mm diameter). Pd was in the form of rod which was cut into tiny pieces. Substrates were borosilicate glass (*Deckglaser* 0.17 mm thick, 24 mm diameter). Hydrogen gas used in the experiments was 99.995% pure.

#### 3.2 Substrate Cleaning

Since the cleanliness of the substrates has a profound effect on the structure and crystallinity of the produced films, it is necessary to eliminate the surface contaminants from the substrates. For this reason before the deposition, substrates were cleaned thoroughly with a seven step treatment using an ultrasonic cleaner (BRANSON 3510). This was 1) substrate cleaning in the heated deionized water for an hour ultrasonically, 2) washing them under normal water for 10 min., 3) cleaning under normal water ultrasonically, 4) rinsing with deionized water, 5) ultrasonic cleaning with deionized water again for 15 min., 6) washing with ethanol, 7) ultrasonic cleaning with ethanol for 15 min. After cleaning process, the substrates have been transferred to thermal evaporation unit immediately to avoid the contamination.

#### 3.3 Thermal Evaporation

##### 3.3.1 Thermal Evaporation Unit

Films were deposited in a custom-made ultra-high vacuum (UHV) thermal evaporation unit designed by Akyıldız et al. 2006. The unit had a stainless steel (304) bell jar with

390 mm height and was connected to base plate (278 mm in diameter, 160 mm in depth) accommodating a total of 12 ports for feedthroughs. A turbo-molecular pump (Adixen ATP150) supported a mechanical dry pump (Adixen ACP15) were connected to the vacuum chamber capable of creating a vacuum level better than  $1 \times 10^{-8}$  mbar monitored with a vacuum gauge (Adixen ACM 2000). The film thickness was monitored and controlled by a thickness quartz single crystal thickness monitor (SQC-310 deposition controller, Sigma Instruments). The unit was also equipped with four power supplies connected to evaporation sources via electrical feedthroughs.

The unit had four resistive evaporation sources equipped with a rotatable shutter above them. An aluminum substrate holder (3 mm thick, 180 mm in diameter) with 25 holes was designed and fixed at a distance 350 mm away from the evaporation sources. A thick copper plate is used as a coolant behind the substrate holder to prevent the excessive heating of the substrates during the evaporation process.

The evaporation unit also accommodated a rotatable macro shutter, rectangular in shape, rotation axes opposite to the Mg source. This allowed controlled exposure of the substrates which by rotating the shutter, substrates in sequence were exposed to the path of evaporation stream (Fig 3.1).

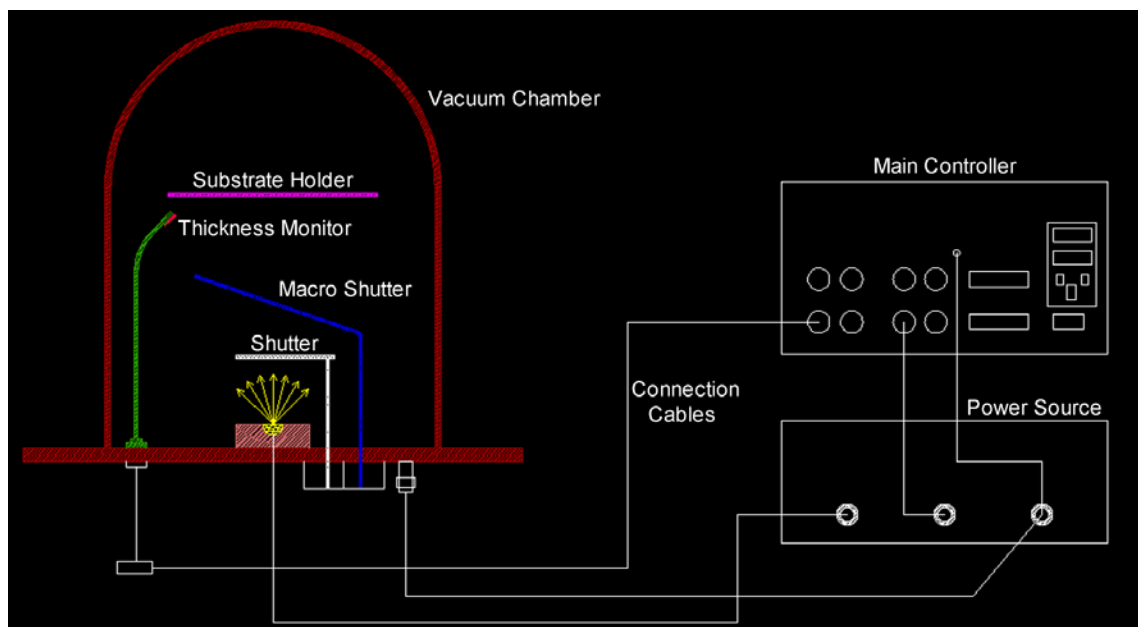


**Fig 3.1** Schematic of the thermal evaporation unit used for the deposition of thin films.

### **3.3.2 Evaporation**

Prior to deposition, cleaned substrates were held in their specified positions on the substrate holder. For evaporation two boats were prepared. One was alumina crucible surrounded by a tungsten heating coil used for Mg granules, and the other was a shallow tantalum boat for Pd chips. Having placed the evaporation materials, the jar was closed and vacuum system was operated. Upon reaching a vacuum level of  $1 \times 10^{-7}$  mbar, experiments were initiated. First, Mg was evaporated with a rate of 10 Å/s and this rate was kept constant as much as possible by changing the current.

Upon reaching a thickness value of 50 nm, initially wide open macro shutter was closed at discreet intervals when the thickness monitor reached values of 100, 150, 200, 300, 400, 500, 600, 800 and 1000 nm. The closing positions used in the evaporation were previously calibrated so that each position yields several samples of the approximately the same thickness.

Having finished the evaporation of Mg, films were coated with a Pd overlayer with a thickness of 20 nm. While Pd was evaporated, the macro shutter was kept wide open so that all films had approximately the same amount of Pd overlayer.

Films were then removed from the thermal evaporator and kept in a glove box (MBRAUN Unilab 1200/780) under the Argon atmosphere.

## **3.4 Resistivity Measurement**

### **3.4.1 Electrical Resistance in Mg/Pd Thin Films**

Upon hydrogenation, conductive Mg converts into a non-conducting MgH<sub>2</sub> phase with high resistivity value. Thus this resistance change could be used to follow sorption process.

A schematic representation of stages in hydride phase formation is given in Fig 3.2. When molecular hydrogen gas is exposed to Mg/Pd thin film, molecular H<sub>2</sub> is adsorbed on the Pd surface and decomposes into atomic H<sub>2</sub>. H<sub>2</sub> in atomic form is able to diffuse

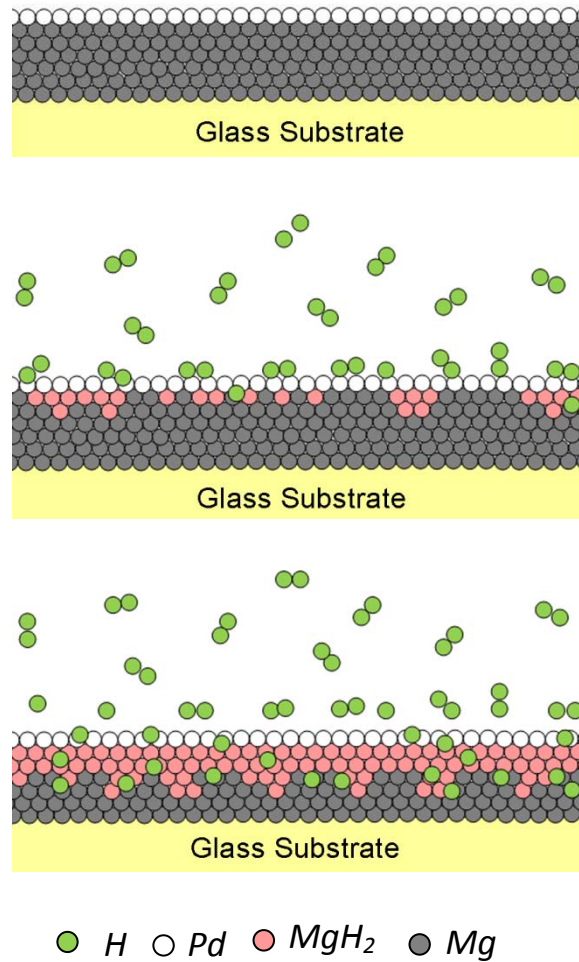


**Fig 3.2** Schematic representation of stages in hydride phase formation.

into the Pd lattice. After passing the Pd layer, hydrogen reaches to Mg/Pd interface and its concentration in this region increases gradually. At early stages of hydrogenation, concentration of the hydrogen in Mg is very low and forms a solid solution with Mg ( $\alpha$ -phase) but with passage of time, the concentration reaches its critical limit and hydride phase with rutile structure ( $\beta$ -phase) nucleates at Mg/Pd interface. Trace amount of hydride phase nuclei within the highly conductive Mg background is not able to affect the conductivity of the film significantly. Further on, numerous nuclei nucleate inside the Mg phase and formerly nucleated nuclei start to grow gradually. Since hydride phase is a semiconductor with relatively large band gap, with growing the hydride phase towards the interior of the film, the resistance of the film starts to increase. With the formation of connected network of hydride phase, unreacted Mg is converted into

islands and as a result a massive change takes place in the resistivity. With the formation of a continuous hydride phase, the hydrogen diffusion through the layer becomes difficult i.e. the film act as self blocking. Therefore, the change in resistivity becomes slower.

The nucleation and growth mechanism given above is reflected to the sigmoidal shape of the resistance vs. temperature curve given in Fig 3.3.

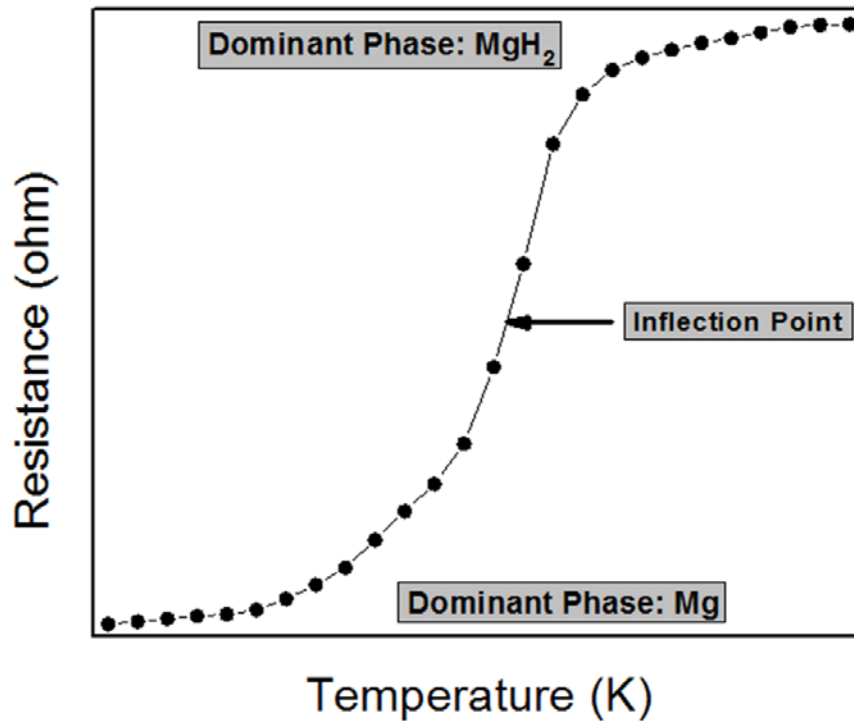


**Fig 3.3** Schematic representation of resistance change as a function of the conversion of Mg to MgH<sub>2</sub>.

Dehydrogenation process, similar to hydrogenation, follows the nucleation and growth mechanism but in the inverse direction. Again, dehydrogenation starts from Mg/Pd interface by nucleating the conductive Mg within semiconducting MgH<sub>2</sub> phase and the desorbed hydrogen is released to external environment via Pd overlayer. With the growth of Mg, the resistance of the film gradually decreases. With the formation of a continuous layer of Mg at the surface, the film becomes conductive and there is a drastic decrease in its resistance. Further decrease in the resistance may be due to the growth of Mg layer.

### 3.4.2 Resistivity Measurement Setup

Resistance measurements were carried out in a setup designed by Özgit et al. 2010. This setup is in the form of a small chamber that allow hydrogenation and dehydrogenation

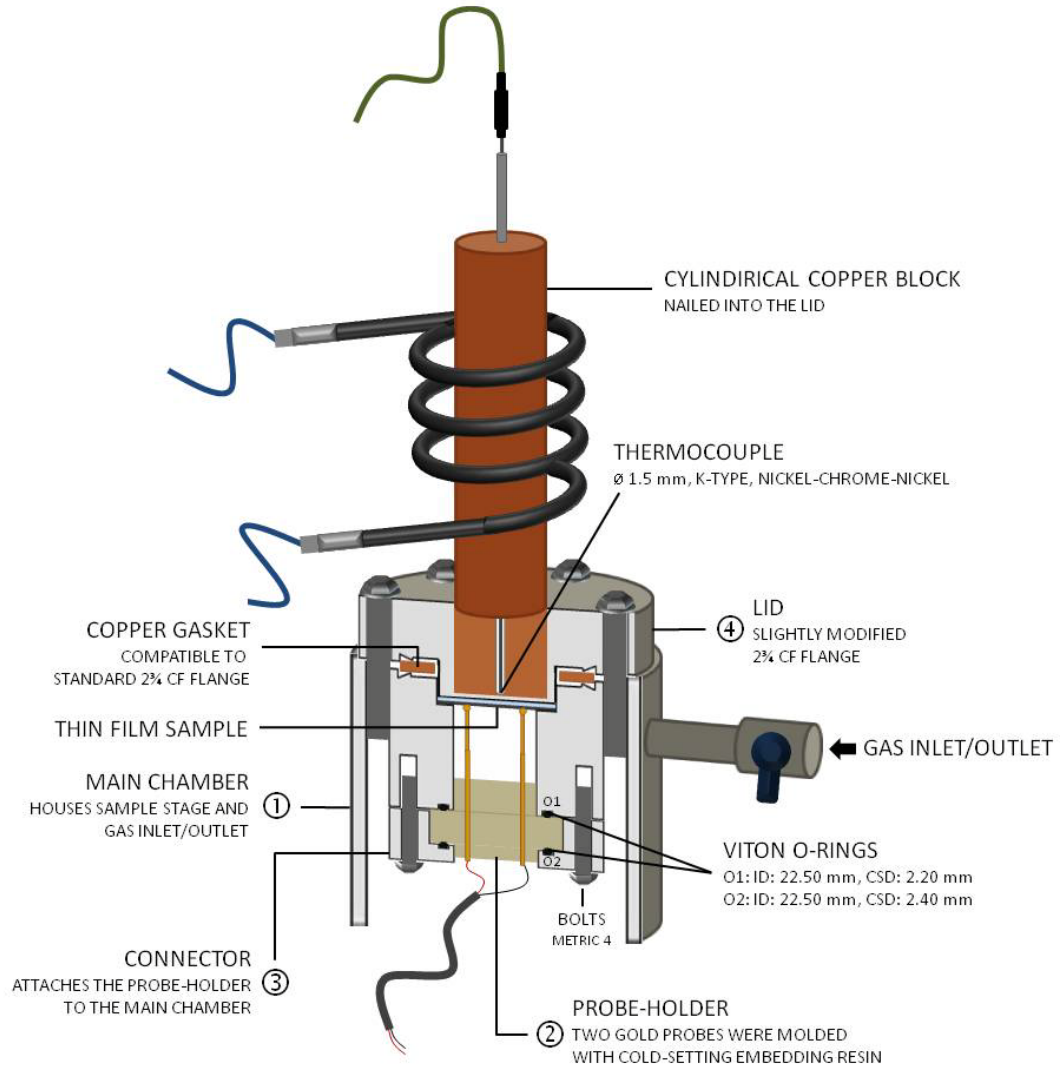


**Fig 3.4** Resistance measurement setup (taken from Özgit 2010).

of the sample while recording the in-situ resistance of the sample. The device could work under H<sub>2</sub> pressure up to 10 bar safely at the temperature range of 298-473 K.

A general schematic of the setup is shown in Fig 3.4. It is composed of four parts: 1) The main chamber which contains the film housing and hydrogen/vacuum entrance tube. 2) The probe holder, composed of two spring loaded gold plated probes (INGUN

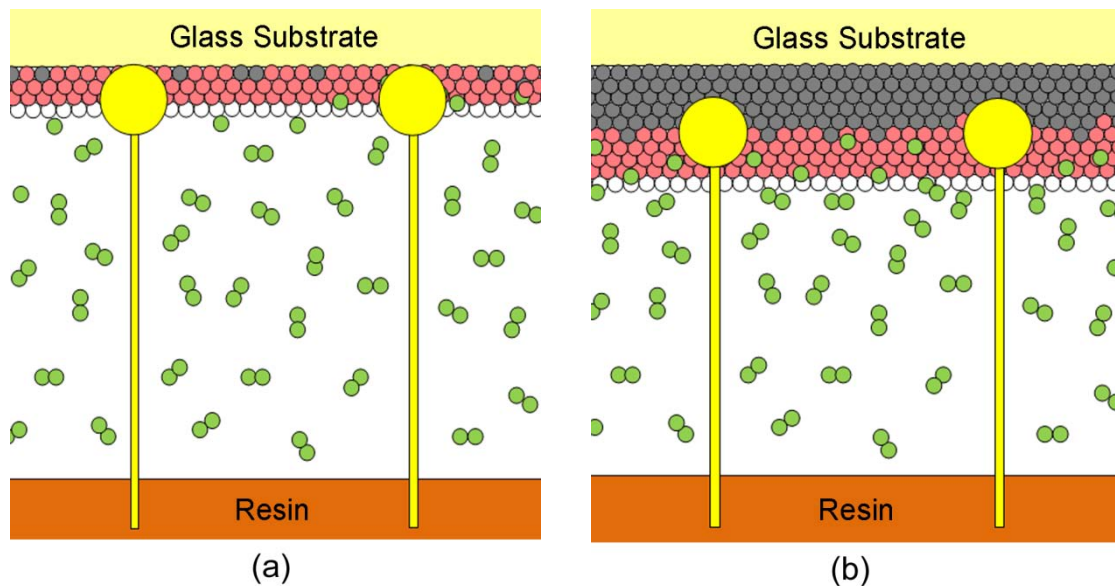


**Fig 3.5** Schematic representation of contacting needles and the thin films. a) needles are in contact with metal hydride only b) needles penetrate deep into the thin film contacting unreacted Mg.

Test Probes, GKS-100-201-90-A) mounted in a cold setting resin. End part of the probes was connected to a Keithley 2700, to read the resistance data, via two copper wires. 3) The connector, to connect the probe holder to the main chamber and 4) the lid of the main chamber. After placing the sample in the setup, the main chamber and the lid fastened to each other tightly using six bolts. A copper gasket was used between the main chamber and the lid to seal the chamber. Pressure inside the chamber was monitored with piezoresistive pressure transmitter (KELLER PAA-23).

Samples were heated under controlled conditions via a heating element surrounding a cylindrical copper rod (27 mm diameter, 200 mm height) which was connected to the lid of the reactor. The heating element was connected to a temperature controller (Tecis PC771) via a solid state relay (GEMO, 25A). Two K-type thermocouples were used for temperature measurement, one of the thermocouples was located close to the sample, and the other was located outside the copper bar near the heating element.

Concerning the setup used for resistance measurement it is important to note that by any reason if the applied force on the gold tips is more than needed value, the needles may pierce the surface layer and penetrate deep into the film. If penetration distance is less than the thickness of hydride layer, Fig 3.5 (a) this penetration is unimportant. However if it is more than the hydride layer the needles would then touch the unreacted Mg with high conductivity Fig 3.5 (b). When this is the case the hydrogenation of the film cannot be followed with the resistance measurement.

The resistance measurement setup is connected to the main hydrogen line (Fig 3.6) to provide the hydrogen gas for absorption experiments and a turbo-molecular pump (Leybold AG PT 50) to evacuate the internal space of the main chamber for desorption experiment.

#### **4.4.3 (De)Hydrogenation Experiments**

(De)Hydrogenation experiments were carried out in a cell which is described in section 3.4.2. Samples were hydrogenated isochronally up to 453 K with a heating rate of 1.5 K/min. and were kept there for 30 min. Two different experimental conditions were used for hydrogenation. For films with thicknesses less than 600 nm, hydrogenation was carried out under a mixed gas (Ar+4%H<sub>2</sub>) with a 90 mbar partial pressure of hydrogen. Films thicker than 600 nm were tested additionally using pure hydrogen gas at a pressure of 2500 mbar.

Following hydrogenation experiments, the samples were cooled down to room temperature while maintaining the applied pressure. The chamber was then taken under vacuum (typically 10<sup>-2</sup> mbar) and the samples were then dehydrogenated. During dehydrogenation, the same heating regime was used, i.e. the chamber was heated to 453 K with a rate of 1.5 K/min.

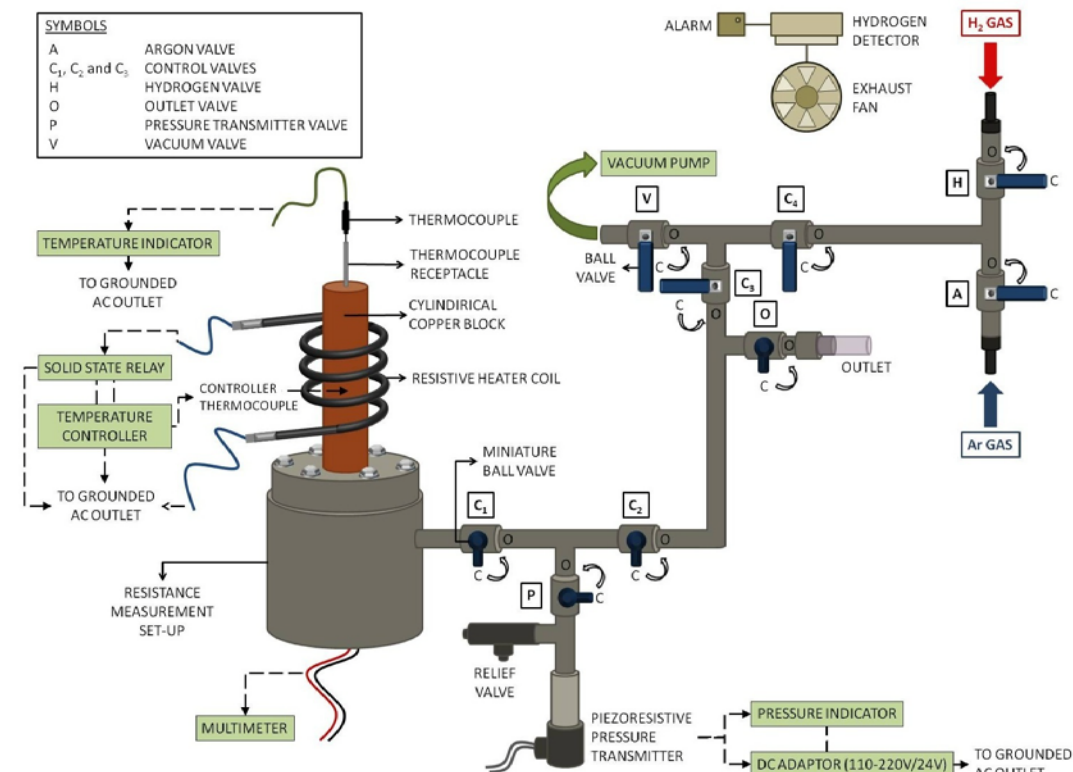


**Fig 3.6** Schematic representation of gas and vacuum feeding system (taken from Özgit 2010)

### 3.5 Characterization of Thin Films

Structural characterization of as-deposited, hydrogenated and dehydrogenated Pd/Mg thin films were carried out with scanning electron microscope (SEM) and XRD. For SEM observations, samples were coated with a thin layer of gold (typically 5 nm thick). XRD were taken using ULTIMA+D/MAX2200/PC Rigaku Diffractometer using CuK<sub>α</sub> radiation with Bragg-Brentano geometry ( $\theta$ - $2\theta$ ) 40 kV and 40 mA. Measurements were taken  $2\theta$  value between 20-80 ° at a rate of 1 °/min. Structural investigations on the films were carried out using FEI 430, Nova NanoSEM. A sample was also investigated with regard to its cell size using transmission electron microscope (TEM) (JEM-2100 LaB6, JEOL).

## CHAPTER 4

### RESULTS AND DISCUSSIONS

#### 4.1 As-deposited State

Mg thin films with thickness values ranging from 50-1000 nm have been deposited on glass substrates. Pd overlayer, nominally 20 nm thick, was applied to the surface of the films to protect them from oxidation and to enhance hydrogen dissociation on the surface. Typical examples of XRD patterns of as-deposited thin films are shown in Fig 4.1. The XRD profiles show that, except 50 nm, thin films have a randomly oriented structure, Mg grains have typically grown (002) parallel to the substrate. Reflection close to  $40^\circ$  was attributed to Pd (111) overlayer.

Figs 4.2 and 4.3 show microstructure in as-deposited thin films. Fig 4.3 (a) and (b) shows the surface morphology of the 200 nm thin film. The structure which has a fish-scale appearance is quite fine with surface grains not larger than 300 nm. The structure in 1000 nm film is much coarser as shown in Fig 4.3 (c) and (d). A bright-field TEM micrograph of the 1000 nm film is given in Fig 4.2. The micrograph refers to a planar section of the film which yields a grain size value of  $\sim 700$  nm. This value is consistent with the size of grains observed in the fish-scale structure given in Fig 4.3 (c) and (d).

Coarseness of the grain structure in 1000 nm thick film may be attributed to overheating of substrate during deposition. Substrates with thicker Mg films are exposed to evaporation source to a longer period of time which, as a result, deposition occurs at elevated temperatures.

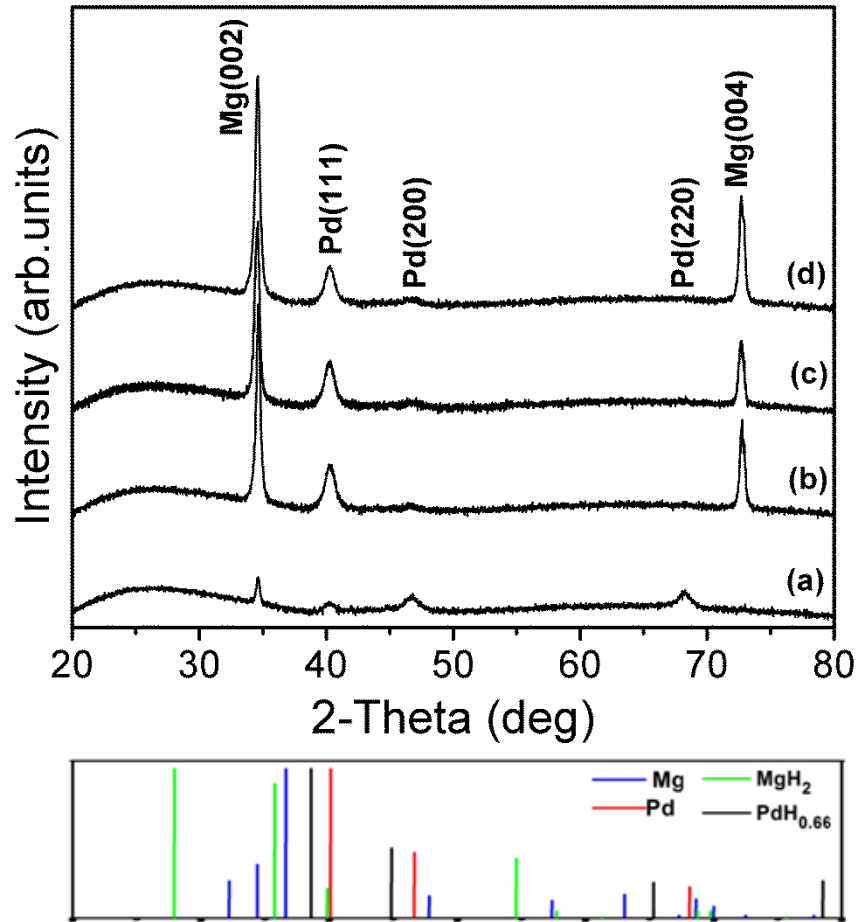


**Fig 4.1** XRD patterns of as-deposited Mg/Pd thin films with thicknesses of a) 50 nm, b) 200 nm, c) 600 nm and d) 1000 nm.

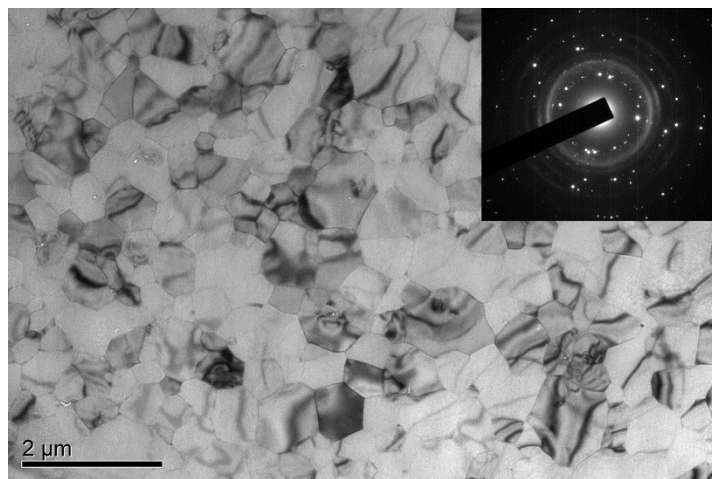


**Fig 4.2** Bright-field TEM micrograph of as-deposited 1000 nm Mg/Pd thin film. The upper inset shows the selected area electron diffraction (SAED) of polycrystalline structure.

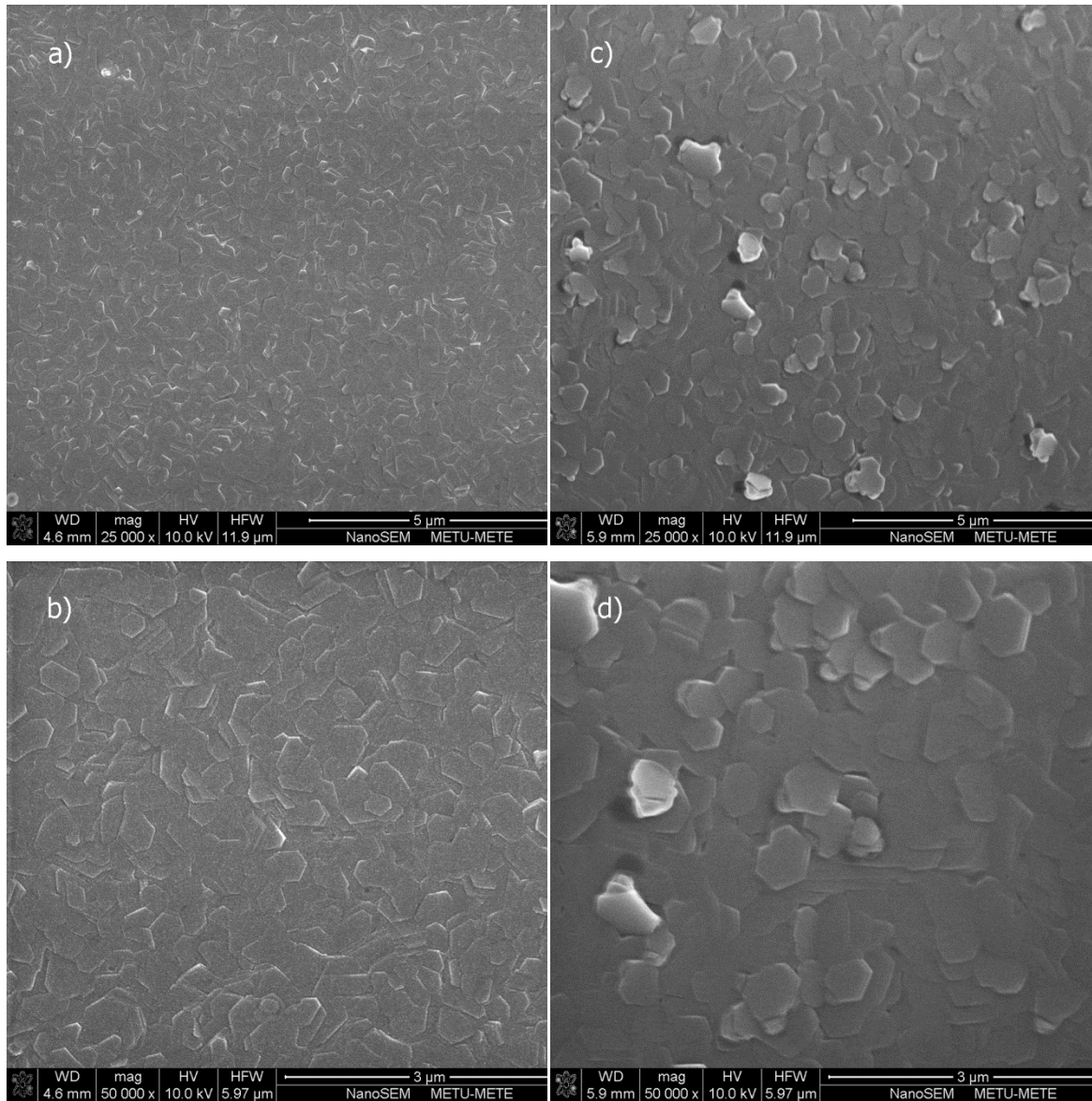


**Fig 4.3** SEM micrographs of as-deposited Mg/Pd thin films with thicknesses of (a,b) 200 nm and (c,d) 1000 nm. Note that the surface grains are much coarser in 1000 nm Mg film.

## 4.2 Hydrogenated State

Thin films were hydrogenated under isochronal condition, i.e. heating with 1.5 K/min. to 453 K. Resistance changes in the thin films recorded during heating are given in Fig 4.4. Hydriding of the film is reflected to an increase in its resistance. Here, it is seen that the resistance rise, i.e. hydrogenation, is postponed to higher temperature with

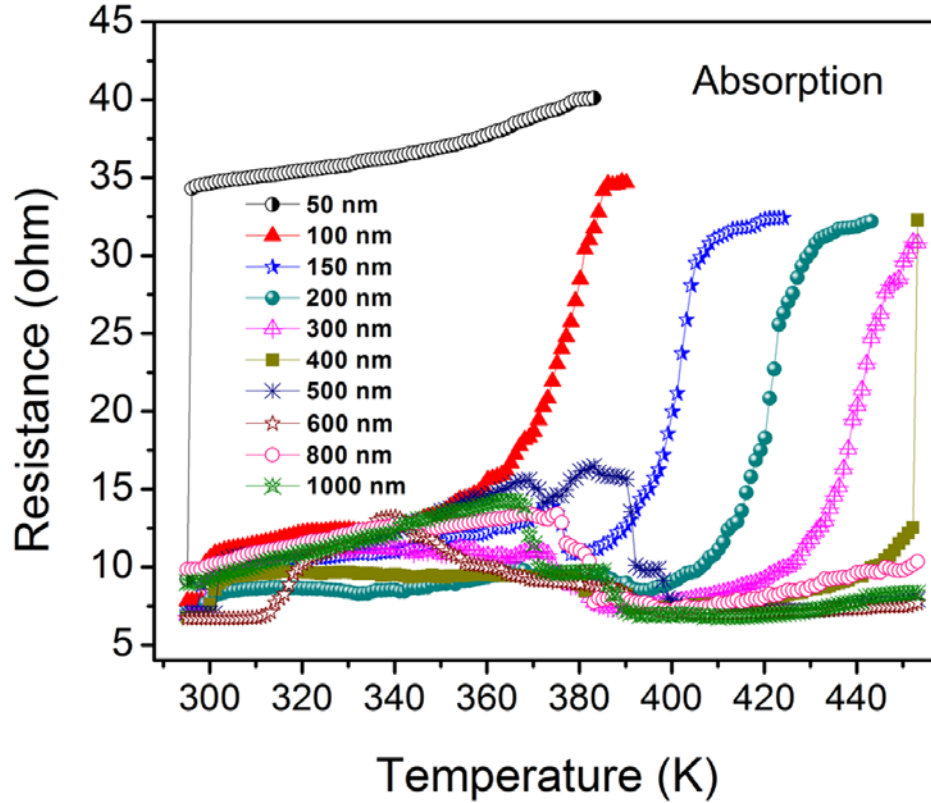


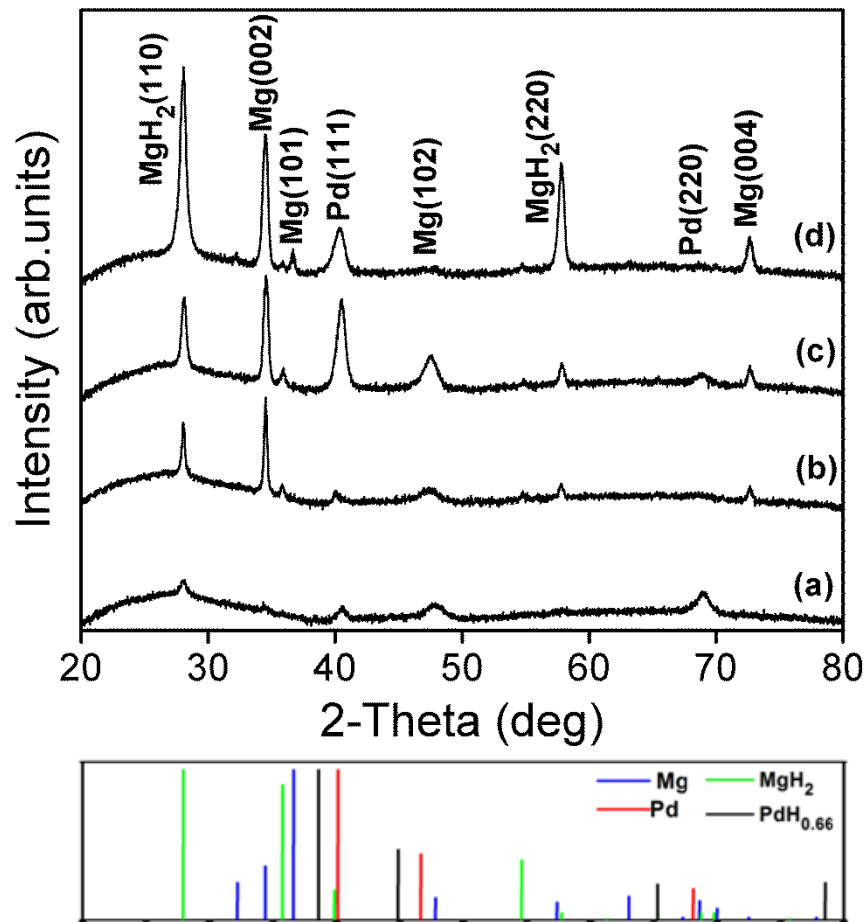
**Fig 4.4** Resistance vs. temperature in isochronal heating of Mg/Pd thin films.

**Table 4.1** Variation of sorption temperatures vs. thickness of the Pd/Mg thin films.

Thickness (nm)	Absorption temp. (K)	Desorption temp. (K)
50	298	405
100	373	415
150	400	420
200	420	423
300	438	440
400	> 453	> 453

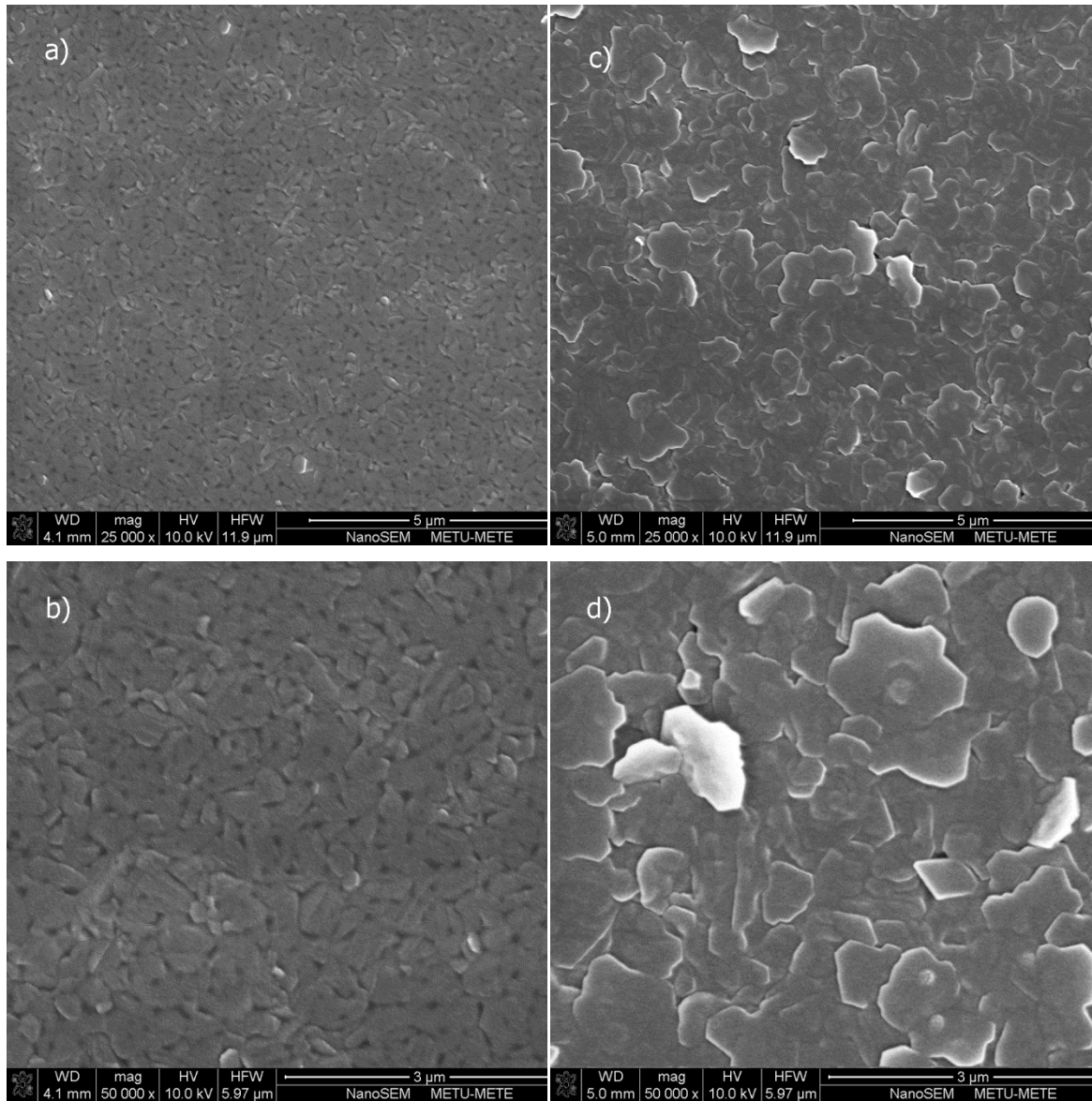
increasing film thickness. Hydrogenation temperature calculated based on the inflection point are tabulated in Table 4.1. It is seen that while 50 nm thin film hydrogenates at room temperature, this value moves to 373 K for 100 nm thin film. The temperature shifts to higher values with increasing thickness reaching a value of 420 K for 200 nm film. Resistance change was followed up to 453 K. Hydrogenation temperatures of films thicker than 300 nm were outside the current measurement range (RT to 453 K).

XRD patterns of the thin films in hydrogenated condition are given in Fig 4.5. It should be noted that, except for very thin films, the pattern comprise both Mg and  $\text{MgH}_2$  peaks. This means that films were partially hydrided since a certain fraction of it remains unreacted. The unreacted portion is quite substantial in thicker films as could be seen in Fig 4.5(d) i.e. 1000 nm thick film, where Mg peaks are particularly dominant.



**Fig 4.5** XRD patterns of Mg/Pd thin films after hydrogenation with thicknesses of a) 100 nm, b) 300 nm, c) 500 nm and d) 1000 nm.

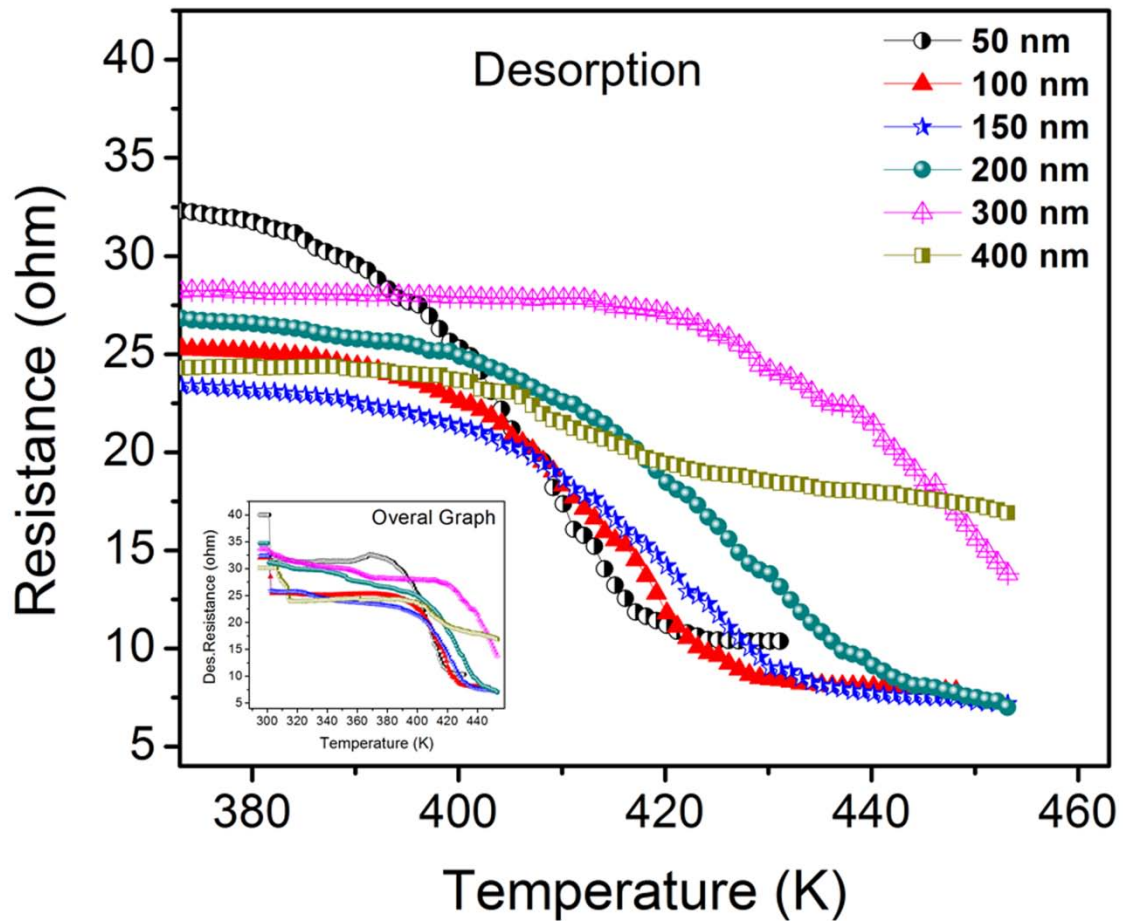
Fig 4.6 shows the microstructure of the 200 and 1000 nm thick films after hydrogenation treatment. The microstructure in both films has pores which formed as a result of hydrogenation.



**Fig 4.6** SEM micrographs of hydrided Mg/Pd thin films with thicknesses of a,b) 200 nm and c,d) 1000 nm.

### 4.3 Dehydrogenated State

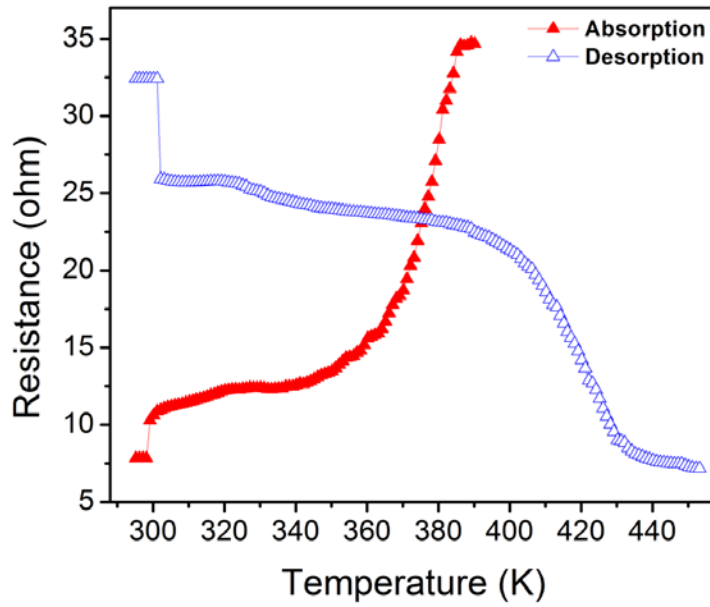
Fig 4.7 shows the dehydrogenation behavior of the films in terms of resistance change. Dehydrogenation temperatures determined based on the inflection point are included in Table 4.1. It is seen that films of thickness values up to 200 nm do dehydrogenate fully before the samples reach 423 K. This is in contrast to thicker films, e.g. 400 nm, which do not dehydrogenate fully as the resistance does not return to their initial values.



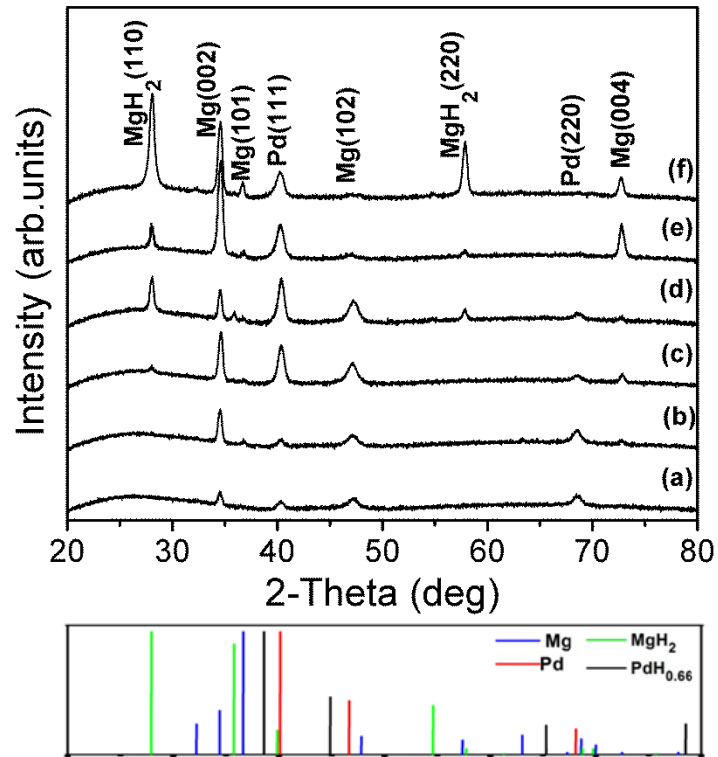
**Fig 4.7** Resistance vs. temperature in isochronal heating of hydrided Mg/Pd thin films under vacuum. See text for details.

Fig 4.8 refers to 100 nm thin film where both hydrogenation and dehydrogenation resistance curves are shown together. It is seen that the temperature at which desorption takes place is higher than the temperature of absorption. It should also be noted that the resistance of the film during desorption returns to the initial resistance value indicating complete desorption of the film.

XRD patterns of dehydrogenated samples are shown in Fig 4.9. Here, it is seen that films up to a thickness of 200 nm contain only Mg peaks. Films thicker than 200 nm in addition to Mg peaks do contain peaks of  $MgH_2$  phase implying that the films did not dehydrogenate fully during the treatment.



**Fig 4.8** Resistance change in absorption and desorption of 100 nm thin film.



**Fig 4.9** XRD patterns of Mg/Pd thin films after dehydrogenation treatment with thicknesses of a) 50 nm, b) 200 nm, c) 300 nm, d) 400 nm, e) 600 nm and f) 1000 nm.

In dehydrogenated condition, drastic change in Mg orientation took place for all film thicknesses. Mg peaks which had mostly (002) orientation now appear with all orientations in XRD patterns. Thus, the film structure was modified as a result of expansion and contraction of the lattice. This is particularly well illustrated in Fig 4.10. This figure refers to 200 nm thin film in as-deposited and after dehydrogenation states. As can be seen in as-deposited state, Mg has a strong (002) reflection. It means that the film structure is highly oriented (002) parallel to the substrate. After dehydrogenation, intensity of the (002) reflection is attenuated and new Mg reflections appear in the diffractogram, implying a random orientation.

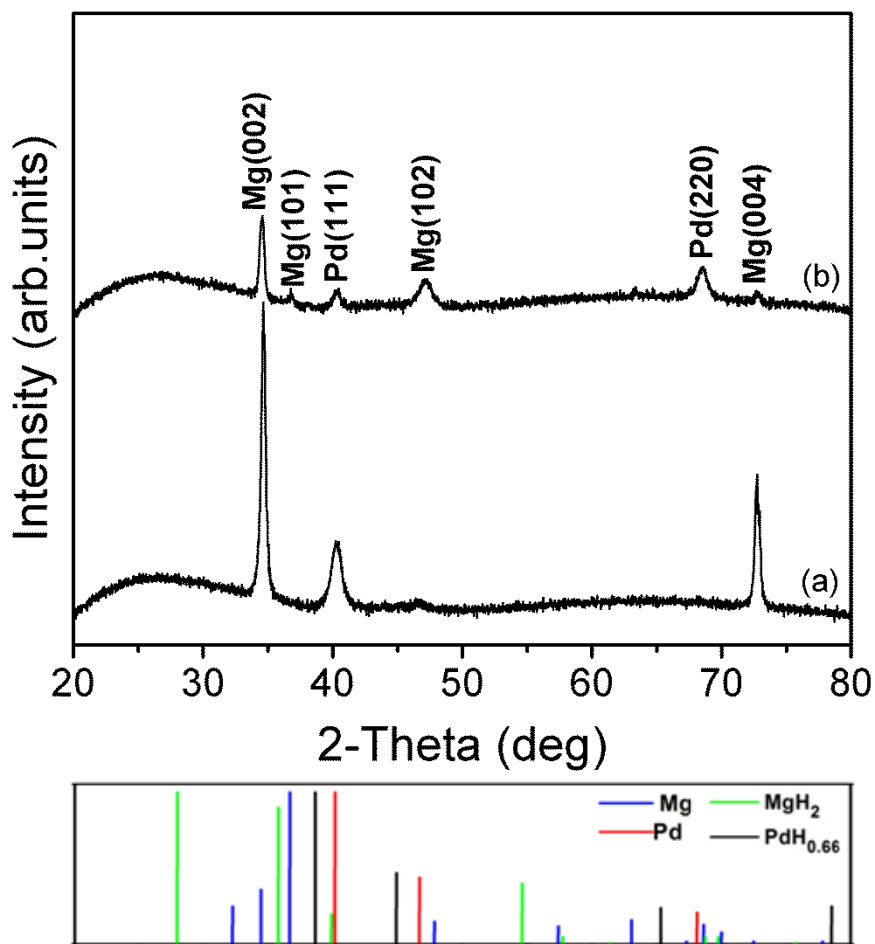


**Fig 4.10** XRD patterns of 200 nm Mg/Pd thin film in a) as-deposited state and b) dehydrogenated state.

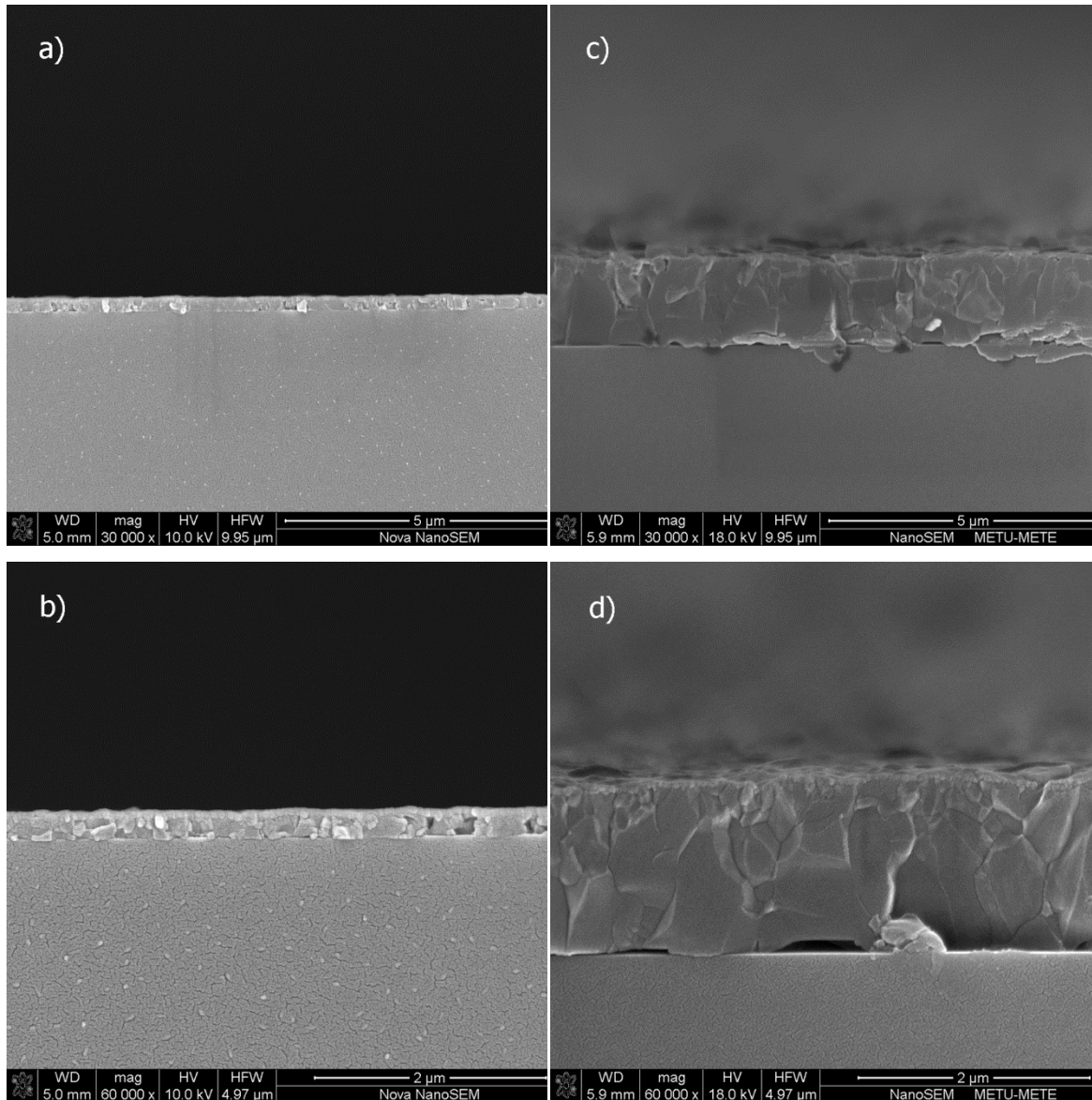
#### 4.4 Microstructural Observations

Fig 4.11 shows the transverse cross-section of hydrogenated films with thicknesses of 200 nm and 1000 nm. Difference in the scale of structure is apparent since both micrographs are recorded at the same magnification. Thicker films have coarse microstructure probably arising as a result of longer exposure to the heat of the evaporation source. It should be noted that there is a morphological similarity between the 200 nm thin film and the upper top layer of 1000 nm film. This morphological observation was also supported by XRD data which show that thicker films hydrogenate only partially.

A similar observation was made by Oguchi et al. 2010 where they studied hydrogenation of wedge shaped Mg-Ti thin film thickness varying from 0 to 500 nm. They observed full hydrogenation in the 120 nm thick surface layer, i.e. the tip was fully hydrogenated while hydrogenation in the rest of the wedge was only partial. Considering that the wedge was hydrided at 373 K, it should be mentioned that this full hydrogenation value of up to 120 nm is consistent with the observations made in the current films, see Fig 4.4.

A typical microstructure of dehydrided film is given in Fig 4.12 (a). This micrograph refers to 1000 nm film. Here it is seen that granulated region which most probably had been hydrided affects only the surface layer. Fig 4.12 (b) refers to a region in different location of the same film. It is seen that granulated regions penetrate to the full thickness of the film. This implies that depth of penetration of hydrogen during hydrogenation is probably structure sensitive. Although there are reports (Akyıldız and Öztürk 2010, Higuchi et al. 2002) which state that refined or amorphous structure facilitate hydrogen diffusion, the current full penetration probably originates from holes in the as-deposited structure which allow hydrogen penetration through its full thickness.

Observations reported above indicate that there is a correlation between the film thickness and the dehydrogenation behavior of thin films. For full dehydrogenation of the films limiting thickness appear to be around 200 nm. It should also be mentioned



**Fig 4.11** Cross-sectional SEM images of hydrided Mg/Pd thin films with thicknesses of a,b) 200 nm and c,d) 1000 nm.

that films up to 200 nm thickness could be hydrogenated and dehydrogenated within a temperature window of up to 423 K. Thicker films hydrogenate and dehydrogenate partially and require the use of temperatures much higher than 423 K.

Since structural defects such as vacancies and grain boundaries were accepted as easy paths for hydrogen diffusion, any factor which decreases their amount will affect the hydrogenation and dehydrogenation properties in a negative way. In addition, during hydrogenation process, Mg phase undergoes a structural change. HCP structure of Mg

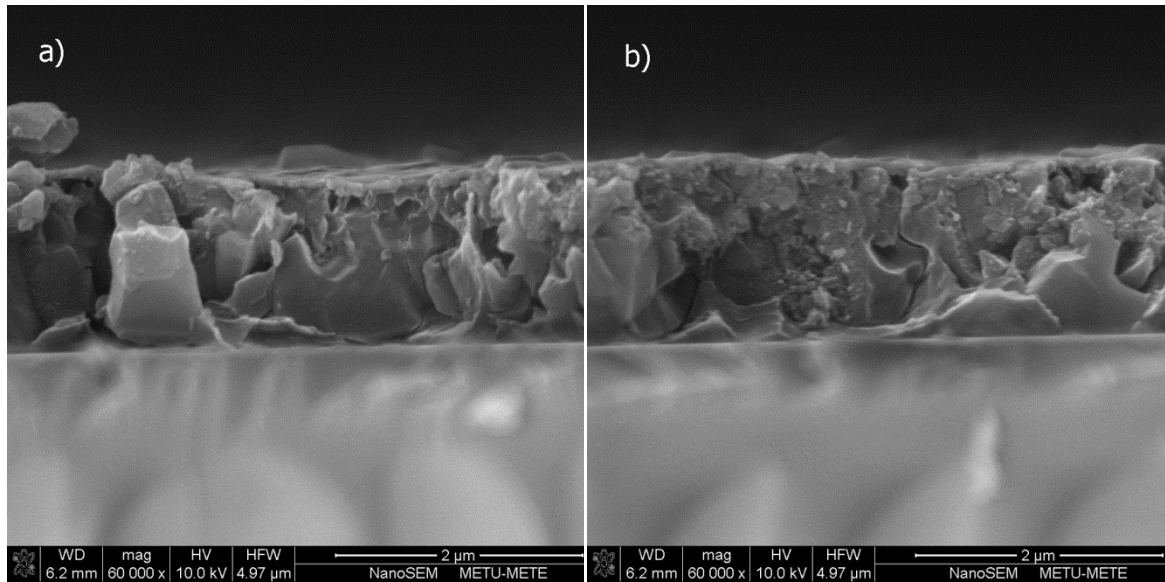


**Fig 4.12** Cross-sectional SEM images of 1000 nm thick film after dehydrogenation. a) Typical cross-section with granulated surface layer. b) Cross-section where the granulated region penetrates to full thickness, see text for details.

converts into body centered tetragonal (BCT) structure of  $\text{MgH}_2$  that is accompanied with considerable volume expansion. In the case of thin films, this volume change mostly takes place in thickness direction.

In films thicker than 200 nm with coarse grain structure, amount of grain boundaries is drastically low. Also hydrogen atom must pass longer distances to reach the lower part of the film to react with Mg. This seems to explain the partial (de)hydrogenation of thicker films.

## CHAPTER 5

### CONCLUSIONS

In this study, effect of film thickness on hydrogenation and dehydrogenation of Mg/Pd thin films were studied. For this purpose, Mg thin films with thickness ranging from 50 to 1000 nm each capped with nominally 20 nm Pd were prepared by a thermal evaporation unit. The unit had a rotatable macro shutter, rectangular in shape, rotation axes opposite to the Mg source, which allowed controlled exposure of the substrates. Thin films of 50, 100, 150, 200, 300, 400, 500, 600, 800 nm and 1000 nm were produced in a single experiment.

Hydrogenation and dehydrogenation behavior of the films were examined using a gas loading chamber which allowed in-situ resistance measurement. Hydrogenation experiments carried out isochronally in the temperature range of 298-453 K with heating rate of 1.5 K/min. Hydrogen gas with chemical composition of (Ar+4% $H_2$ ) and partial pressure of 90 mbar was used for hydrogenation process. In addition, pure  $H_2$  gas with 2500 mbar partial pressure was used for films thicker than 600 nm in thickness. Dehydrogenation treatments carried out at the same temperature range with the same heating regime but under vacuum condition ( $\sim 10^{-2}$  mbar).

The study has shown the followings:

- 1) Thin film with 50 nm thickness has random texture in the as-deposited state, whereas thicker films have preferred orientation (002) plane parallel to the substrate.
- 2) Mg/Pd thin films of up to 200 nm hydrogenate fully and the hydrogenation temperature shifts to higher temperatures with film thickness. Films thicker than 200 nm hydrogenate only partially, considerable portion of the film remains unreacted. Similarly,

3) Films up to 200 nm dehydrogenate fully at relatively low temperatures i.e.  $\leq 423$  K. The thicker films require the use of higher dehydrogenation temperatures and the desorption is only partial.

To what extent the above observation is applicable to powders is not known since the film behavior is not necessarily the same as the powder behavior. Assuming that they are similar, the current study implies that for efficient hydrogen storage, it is necessary to aim for a powder size of less than 400 nm.

## REFERENCES

- Akyıldız H and Öztürk T, 2010, “*Hydrogen sorption in crystalline and amorphous Mg–Cu thin films*”, J. Alloy. Compd. 492: 745–750.
- Akyıldız H, Özenbaş M, Öztürk T, 2006, “*Hydrogen absorption in magnesium based crystalline thin films*”, Int. J. Hydrogen Energ. 31:1379-1383.
- Ares JR, Leardini F, Díaz-Chao P, Bodega J, Koon DW, Ferrer IJ, Fernández JF, Sánchez C, 2010, “*Hydrogen desorption in nanocrystalline MgH<sub>2</sub> thin films at room temperature*”, J. Alloy. Compd. 495:650–654.
- Barcelo S, Rogers M, Grigoropoulos CP, Mao SS, 2010, “*Hydrogen storage property of sandwiched magnesium hydride nanoparticle thin film*”, Int. J. Hydrogen Energ. 35:7232-7235.
- Bogdanovic´ B, Bohmhammel K, Christ B, Reiser A, Schlichte K, Vehlen R , Wolf U, 1999, “*Thermodynamic investigation of the magnesium–hydrogen system*”, J. Alloy. Compd. 282:84–92.
- Bouhtiyya S and Roue´ L, 2009, “*Pd/Mg/Pd thin films prepared by pulsed laser deposition under different helium pressures: Structure and electrochemical hydriding properties*”, Int. J. Hydrogen Energ. 34:5778-5784.
- Chacon C, Johansson E, Hjörvarsson B, Zlotea C, Andersson Y, 2005, “*Growth and hydrogen uptake of Mg–Y thin films*”, J. Appl. Phys. 97:104903-7.

Domènech-Ferrer R , Sridharan MG, Garcia G, Pi F, Rodríguez-Viejo J, 2007, “*Hydrogenation properties of pure magnesium and magnesium–aluminium thin films*”, J. Power Sources 169:117–122.

Dornheim M, Doppiu S, Barkhordarian G, U. Boesenberg U, Klassen T, Gutfleisch O, Bormann R, 2007, “*Hydrogen storage in magnesium-based hydrides and hydride composites*”, Scripta Mater. 56:841–846.

Dornheim M, S. Doppiu S, Barkhordarian G, Boesenberg U, Klassen T, Gutfleisch O, Bormann R, 2007, “*Hydrogen storage in magnesium-based hydrides and hydride composites*”, Scripta Mater. 56:841–846.

Fujii H and Orimo S, 2003, “*Hydrogen storage properties in nano-structured magnesium- and carbon-related materials*”, Physica B 328:77–80.

Gautam YK, Chawla AK, Walia R, Agrawal RD, Ramesh Chandra R, 2011, “*Hydrogenation of Pd-capped Mg thin films prepared by DC magnetron sputtering*”, Appl. Surf. Sci. 257:6291–6295.

Grau-Crespo R, Smith KC, Fisher TS, de Leeuw NH, Waghmare UV, 2009, “*Thermodynamics of hydrogen vacancies in MgH<sub>2</sub> from first-principles calculations and grand-canonical statistical mechanics*”, Phys. Rev. B 80:174117.

Higuchi K, Kajioka H, Toiyama K, Fujii H, Orimo S, Kikuchi Y, 1999, “*In situ study of hydriding–dehydriding properties in some Pd/Mg thin films with different degree of Mg crystallization*”, J. Alloy. Compd. 293–295:484–489.

Higuchi K, Yamamoto K, Kajioka H, Toiyama K, Honda M, S. Orimo S, Fujii H, 2002, “*Remarkable hydrogen storage properties in three-layered Pd/Mg/Pd thin films*”, J. Alloy. Compd. 330–332:526–530.

Hjort P, Krozer A, Kasemo B, 1996a, “*Resistivity and hydrogen uptake measurements in evaporated Mg films at 350 K*”, J. Alloy. Compd. 234: L11-L15.

Hjort P, Krozer A, Kasemo B, 1996b, “*Hydrogen sorption kinetics in partly oxidized Mg films*”, J. Alloy. Compd. 237: 74-80.

Ingason AS and Olafsson S, 2005, “*Thermodynamics of hydrogen uptake in Mg films studied by resistance measurements*”, J. Alloy. Compd. 404–406:469–472.

Kelekar R, Giffard H, Kelly ST, Clemens BM, 2007, “*Formation and dissociation of MgH<sub>2</sub> in epitaxial Mg thin films*”, J. Appl. Phys. 101, 114311.

Kelly ST and Clemens BM, 2010, “*Moving interface hydride formation in multilayered metal thin films*”, J. Appl. Phys. 108, 013521-6.

Krozer A and Kasemo B, 1987, “*Unusual kinetics due to interface hydride formation in the hydriding of Pd/Mg sandwich layers*”, J. Vac. Sci. Technol. A 5 (4):1003-1005.

Krozer A and Kasemo B, 1989, “*Equilibrium hydrogen uptake and associated kinetics for the Mg-H<sub>2</sub> system at low pressures*”, J. Phys-Condens. Mat. 1: 1533-1538.

Krozer A and Kasemo B, 1990, “*Hydrogen uptake by Pd-coated Mg: Absorption-decomposition isotherms and uptake kinetics*”, J. Less-Common Met. 160: 323-342.

Kumar S, Reddy GLN, Raju VS, 2009, “*Hydrogen storage in Pd capped thermally grown Mg films: Studies by nuclear resonance reaction analysis*”, J. Alloy. Compd. 476:500–506.

Léon A, Knystautas EJ, Huot J, Schulz R, 2002, “*Hydrogenation characteristics of air-exposed magnesium films*”, J. Alloy. Compd. 345:158–166.

Lohstroh W, Westerwaal RJ, Van Mechelen JLM, Chacon C, Johansson E, Dam B, Griessen R, 2004, “ *Structural and optical properties of Mg<sub>2</sub>NiH<sub>x</sub> switchable mirrors upon hydrogen loading*”, Phys. Rev. B 70, 165411-11.

Oguchi H, Tan Z, Heilweil EJ, Bendersky LA, 2010, “*In-situ infrared imaging methodology for measuring heterogeneous growth process of a hydride phase*”, Int. J Hydrogen Energ. 35:1296-1299.

Ostenfeld CW and Chorkendorff I, 2006, “*Effect of oxygen on the hydrogenation properties of magnesium films*”, Surf. Sci. 600:1363–1368.

Ostenfeld CW, Johansson M, Chorkendorff I, 2007, “*Hydrogenation properties of catalyzed and non-catalyzed magnesium films*”, Surf. Sci. 601:1862–1869.

Özgit Ç, Akyıldız H, Öztürk T, 2010, “*Isochronal hydrogenation of textured Mg/Pd thin films*”, Thin Solid Films 518:4762–4767.

Paillier J and Roue L, 2005, “*Hydrogen electrosorption and structural properties of nanostructured Pd–Mg thin films elaborated by pulsed laser deposition*”, J. Alloy. Compd. 404–406:473–476.

Pasturel M, Slaman M, Schreuders H, Rector JH, Borsa DM, Dam B, Griessen R, 2006, “*Hydrogen absorption kinetics and optical properties of Pd-doped Mg thin films*”, J. Appl. Phys. 100:023515-8.

Pranevicius L, Milcius D, Templier C, Pranevicius LL, Lelis M, 2009, “*Studies of Mg film and substrate coupling effects on hydrogenation properties*”, J. Alloy. Compd. 488:360–363.

Qu J, Sun B, Liu Y, Yang R, Li Y, Li X, 2010, “*Improved hydrogen storage properties in Mg-based thin films by tailoring structures*”, Int. J. Hydrogen Energ. 35:8331-8336.

Qu J, Sun B, Yang R, Zhao W, Wang Y, Li X, 2010, “*Hydrogen absorption kinetics of Mg thin films under mild conditions*”, Scripta Mater. 62:317–320.

Qu J, Sun B, Zheng J, Yang R, Wang Y, Li X, 2010, “*Hydrogen desorption properties of Mg thin films at room temperature*”, J. Power Sources 195:1190–1194.

Qu J, Wang Y, Xie L, Zheng J, Liu Y, Li X, 2009, “*Hydrogen absorption–desorption, optical transmission properties and annealing effect of Mg thin films prepared by magnetron sputtering*”, Int. J. Hydrogen Energ. 34:1910-1915.

Qu J, Wang Y, Xie L, Zheng J, Liu Y, Li X, 2009, “*Superior hydrogen absorption and desorption behavior of Mg thin films*”, J. Power Sources 186: 515–520.

Reddy GLN, Kumar S, Sunitha Y, Kalavathi S, Raju VS, 2009, “*Intermixing and formation of Pd–Mg intermetallics in Pd/Mg/Si films*”, J. Alloy. Compd. 481:714–718.

Richardson TJ, Farangis B, Slack JL, Nachimuthu P, Perera R, Tamura N, Rubin M, 2003, “*X-Ray absorption spectroscopy of transition metal–magnesium hydride thin films*”, J. Alloy. Compd. 356–357:204–207.

Rydén J, Hjörvarsson B, Ericsson T, Karlsson E, Krozer A, Kasemo B, 1989, “*Unusual kinetics of hydride formation in Mg-Pd sandwiches, studied by hydrogen profiling and quartz crystal microbalance measurements*”, J. Less-Common Met. 152:295-309.

Schlapbach L and Züttel A, 2001, “*Hydrogen-storage materials for mobile applications*”, Nature 414:353-358.

Shalaan E and Schmitt H, 2006, “*Mg nanoparticle switchable mirror films with improved absorption–desorption kinetics*”, Surf. Sci. 600:3650–3653.

- Singh S, Eijt SWH, Zandbergen MW, Legerstee WJ, Svetchnikov VL, 2007, “*Nanoscale structure and the hydrogenation of Pd-capped magnesium thin films prepared by plasma sputter and pulsed laser deposition*”, J. Alloy. Compd. 441:344–351.
- Siviero G, Bello V, Mattei G, Mazzoldi P, Battaglin G, N. Bazzanella N, Checchetto R, Miotello A, 2009, “*Structural evolution of Pd-capped Mg thin films under H<sub>2</sub> absorption and desorption cycles*”, Int. J. Hydrogen Energ. 34:4817-4826.
- Spatz P, Aebischer HA, Krözer A, Schlapbach L, 1993, “*The diffusion of H in Mg and the nucleation and growth of MgH<sub>2</sub> in thin-films*”, Z Phys. Chem 181:393-397.
- Sunitha Y, Reddy GLN, Kumar S, Raju VS, 2009, “*Studies on interdiffusion in Pd/Mg/Si films: Towards improved cyclic stability in hydrogen storage*”, Appl. Surf. Sci. 256:1553–1559.
- Tamboli SH, Puri V, R.K. Puri RK, 2010, “*Adhesion and stress of magnesium oxide thin films: Effect of thickness, oxidation temperature and duration*”, Appl. Surf. Sci. 256:4582–4585.
- Vermeulen P, Ledovskikh A, Danilov D, Notten PHL, 2009, “*Thermodynamics and kinetics of the thin film magnesium–hydrogen system*”, Acta Mater. 57:4967–4973.
- Westerwaal RJ, Broedersz CP, Gremaud R, Slaman M, Borgschulte A, Lohstroh W, Tschersich KG, Fleischhauer HP, Dam B, Griessen R, 2008, “*Study of the hydride forming process of in-situ grown MgH<sub>2</sub> thin films by activated reactive evaporation*”, Thin Solid Films 516:4351–4359.
- Yamamoto K, Higuchi K, Kajioka H, Sumida H, Orimo S, Fujii H, 2002, “*Optical transmission of magnesium hydride thin film with characteristic nanostructure*”, J. Alloy. Compd. 330–332:352–356.

Ye SY, Chan SLI, Ouyang LZ, M. Zhu M, 2010, “*Hydrogen storage and structure variation in Mg/Pd multi-layer film*”, J. Alloy. Compd. 504:493–497.

Yoshimura K, Yamada Y, Okada M, 2004, “*Hydrogenation of Pd capped Mg thin films at room temperature*”, Surf. Sci. 566–568:751–754.

Zaluska A and Zaluski L, Ström–Olsen JO, 1999, “*Nanocrystalline magnesium for hydrogen storage*”, J. Alloy. Compd. 288:217–225.